Title	Pyridine-derived N-heterocyclic carbenes: An experimental and theoretical evaluation of the bonding in and reactivity of selected normal and abnormal complexes of Ni(II) and Pd(II)
Authors(s)	Stander-Gobler, Elzet, Schuster, Oliver, Cronje, Stephanie, Tosh, Evangeline, Albrecht, Martin, Frenking, Gernot, Raubenheimer, Helgard G., Heydenrych, Greta
Publication date	2010-10-22
Publication information	Stander-Gobler, Elzet, Oliver Schuster, Stephanie Cronje, Evangeline Tosh, Martin Albrecht, Gernot Frenking, Helgard G. Raubenheimer, and Greta Heydenrych. "Pyridine-Derived N-Heterocyclic Carbenes: An Experimental and Theoretical Evaluation of the Bonding in and Reactivity of Selected Normal and Abnormal Complexes of Ni(II) and Pd(II)." ACS, October 22, 2010. https://doi.org/10.1021/om100431u.
Publisher	ACS
Item record/more information	http://hdl.handle.net/10197/3880
Publisher's version (DOI)	10.1021/om100431u

Pyridine-derived N-heterocyclic carbenes: An experimental and theoretical evaluation of the bonding in and reactivity of selected normal and abnormal complexes of Ni(II) and Pd(II)

Elzet Stander-Grobler[a], Oliver Schuster[a,d,*], Greta Heydenrych[b], Stephanie Cronje,[a]
Evangeline Tosh[c], Martin Albrecht[d], Gernot Frenking[b,*], Helgard G. Raubenheimer[a,*]

[a] Department of Chemistry and Polymer Science, University of Stellenbosch, Private Bag X1, Matieland, 7602, Stellenbosch, South Africa.

[b] Fachbereich Chemie, Philipps-Universität Marburg, Hans-Meerwein-Strasse, D-35043 Marburg.

[c] Inorganic Chemistry Department, Technische Universität München, Lichtenbergstr. 4, D-85747 Garching.

[d] Department of Chemistry, University of Fribourg, Chemin du Musée 9, CH-1700 Fribourg.

Abstract

We report a thorough investigation of a series of isomeric complexes with the general formula *trans*-(pyridylidene)M$(PPh_3)_2$Cl (M = Pd, Ni). For the first time, a systematic comparison of *normal*, *abnormal* and *remote* bonding modes is presented. X-ray structural and ^{13}C NMR data indicate the importance of carbenoid mesomeric contributions in their compound class. The catalytic performance of the palladium complexes, *trans*-(pyridylidene)Pd$(PPh_3)_2$Cl, as precursors in Suzuki-Miyaura-type cross-coupling suggests a correlation of *remote* bonding with catalyst robustness and thus effectivity. When metal precursors $M(PPh_3)_4$ are reacted with 2,4-dichloro pyridinium salts, preferential formation of *remote* carbene complexes occurs and indications are that electronic parameters rather than steric influences are responsible for the observed selectivity. Calculations at the BP86/TZ2P level of theory support interpretation of the results.

Introduction

The chemistry of N-heterocyclic carbenes (NHCs) has seen an explosive development during the last number of years.[1-5] However, despite the vast number of possible N-heterocycles that could be classified as carbenes, the activity in NHC chemistry has concentrated by and large on 2-imidazolylidenes - often called 'Arduengo'-carbenes.[1-5] Only recently it has been shown that an abnormal binding mode via the C4 (or C5) position of imidazolylidenes yields extraordinary electron rich metal centers.[6-17] These discoveries led to a considerably increased interest in "non-classical" NHCs, *i.e.* carbenes that are not stabilized by two adjacent heteroatoms.[18] We have been active in this field for a decade and have investigated in particular pyridinium-derived carbenes.[19-25] With now well-established protocols for the functionalization of pyridine, pyridylidenes offer great potential for variation of steric demand and electronic properties. Moreover, they can bind to the metal in a *normal* (**I**, **III**) or *abnormal* (**II**) fashion (Scheme 1) with the possibility of both normal and abnormal carbenes arising in a *remote* position. We have extended Crabtree's terminology[6,7] by using the term *abnormal* whenever it is not possible to illustrate the carbene structure without charge separation (in contrast to **Ia** and **IIIa**).[18] *Remote* denotes a carbene that contains no stabilizing heteroatom directly adjacent to the carbene carbon. Accordingly, isomer **II** is *abnormal* and *remote*, whereas isomer **III** is *normal* and *remote*.

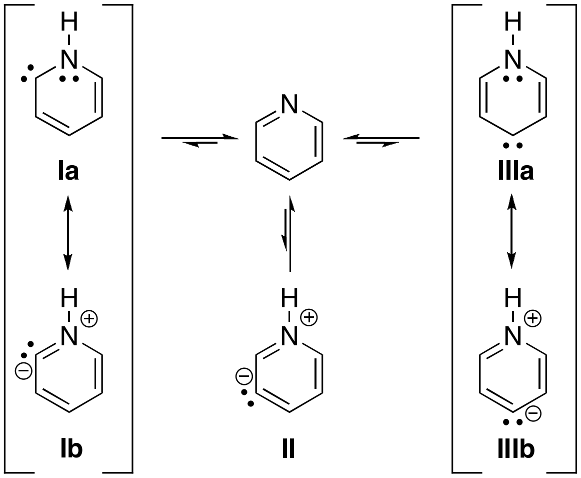

Scheme 1. Isomeric pyridine and pyridylidenes.

Previous theoretical investigations of the *free* ligands, indicate that pyridine is by far more stable (0.0 kcal/mol) than the most stable carbenoid isomer **I** (ca. 40 kcal mol^{-1}) while the *remote* species **II** and **III** are even higher in energy (both ca. 55 kcal mol^{-1}).[24,26,27] Interestingly, calculations of isodesmic reactions by Kassaee *et al.* suggest a similar stabilization of the methylene fragment in 2- and 4-pyridylidenes.[28] Significant barriers for *intra*molecular interconversion allowed for detecting the co-existence of isomers **I** and **II** under high vacuum conditions.[26,27] In the condensed phase, *inter*molecular interconversion is more facile and pyridylidenes have thus far only been observed in complexes, *i.e.* stabilized by a metal center.[29] Such metal-stabilized pyridylidenes have been accessible in a few cases by a ligand isomerization process involving a formal proton shift from carbon to nitrogen. Depending on the ring substitution pattern, both 2- and 4-pyridylidene complexes have been prepared by such a rearrangement.[30-34] In contrast, C-H activation of N-*alkylated* pyridinium precursors that could allow for C2- or C4-coordination, exclusively leads to metallation at the 4-position.[35-39] This observation has been attributed to the steric bulk of the N-alkyl group.

We first carried out a thorough investigation of a series of isomeric complexes with the general formula *trans*-(pyridylidene)M$(PPh_3)_2$Cl (M = Pd, Ni) using various experimental and computational parameters. We were particularly interested in evaluating whether certain mesomeric contributions would be particularly significant and if the concept of *abnormal* carbene bonding, which is defined on the basis of simple valence bond considerations, transfers to experimental observations. Secondly, the catalytic performance of the palladium complexes *trans*-(pyridylidene)Pd$(PPh_3)_2$Cl as precursors in Suzuki-Miyaura-type cross-coupling reactions was studied in order to elucidate the influence of *normal*, *abnormal*, or *remote* carbene bonding. Finally, we investigated preferential carbene complex formation by oxidative addition using low-valent metal precursors and 2,4-dichloro pyridinium salts. DFT calculations were used to support our interpretation of the results. As an extension of our studies on quinolylidene complexes,[20,21,23,40-42] we also determined the reactivity of M$(PPh_3)_4$ (M = Pd, Ni) towards 4,7-dichloroquinolinium salts, wherein both chloro substituents are located three bonds away from the nitrogen atom.

Throughout the manuscript, carbene complexes are drawn with a M=C double bond if applicable. Our choice of representation should not be regarded as a statement concerning the actual bonding. It merely helps the reader to identify formal (normal) carbene metal bonds.

Results and Discussion

a) Synthesis of 2-, 3-, and 4-Pyridylidene Metal Complexes

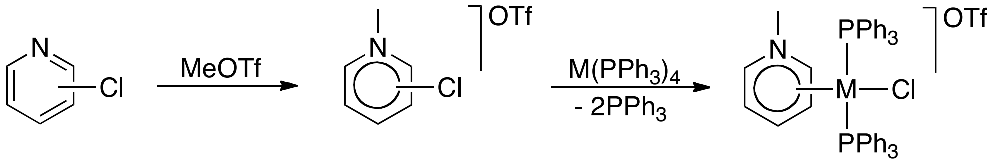

1a (2-pyridyl)
b (3-pyridyl)
c (4-pyridyl)

2

3 (M = Pd)
4 (M = Ni)

Scheme 2: Preparation of two complete series of carbene complexes.

The synthetic routes used to prepare two complete series of ionic 2-, 3-, and 4-pyridylidene metal complexes **3** and **4** are summarized in Scheme 2 and follow our established strategy which has been reported earlier.[23] Pyridinium triflates **2** (triflate = OTf = trifluoromethanesulphonate) were prepared from the corresponding chloropyridines **1a-c** with one equivalent of methyltriflate in dry dichloromethane. Subsequent oxidative addition of the ligand precursor salts to $Ni(PPh_3)_4$ in THF at room temperature afforded the desired yellow cationic complexes **4** in good yields. Similar procedures in toluene at 60°C were followed to obtain the corresponding colorless palladium complexes **3**. The oxidative addition leading to the *abnormal* complex **3b** occurred significantly slower than the corresponding reaction for *normal* carbenes.

b) Single crystal structure determinations

The ORTEP drawing of the molecular structure of the nickel complex **4b** in Figure 1 is representative for the square planar geometry generally observed for complexes **3** and **4**, as previously established for BF_4-analogues of the 2- and 4-pyridylidene metal complexes.[20,21] The phosphine ligands adopt the usual *trans* configuration. Unlike the corresponding complexes **3a** and **4a** or **3c** and **4c** (in the BF_4-salt), which crystallize in distinct packing arrangements,[20,21] crystals of **3b** and **4b** (in the OTf-salt) are isomorphous. Relevant parameters for the entire series of isomeric cationic structures are summarized in Table 1.

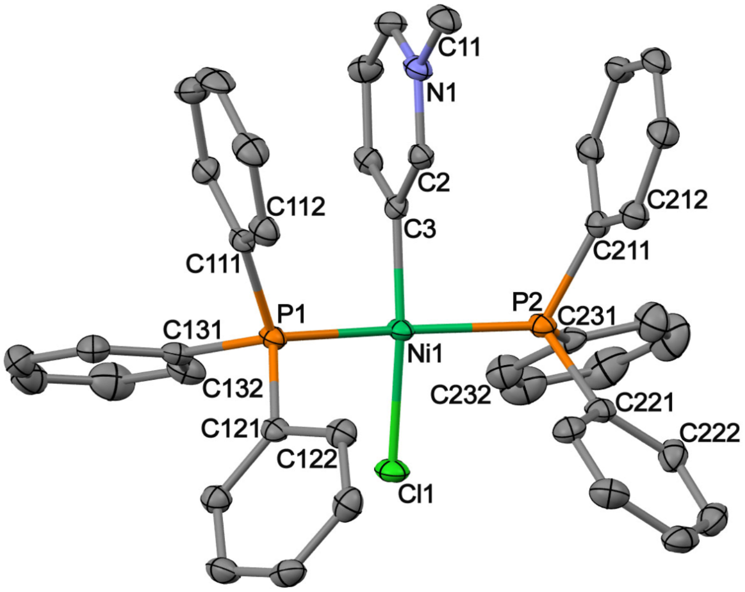

Figure 1: Molecular structure of the cationic complex **4b** (50% probability ellipsoids, hydrogen atoms and counterion omitted)

Table 1: Selected structural parameters of the series of pyridylidene complexes

	d (M-C) [Å]	d (M-Cl) [Å]	CCX angle [°]	Torsion[a] [°]	Distortion[b] [Å]
3a	2.002(3)[c]	2.3638(8)	116.22[c]	88.60[c]	0.628[c]
3b	1.996(7)	2.371(2)	117.82	88.21	0.572
3c[d]	1.979(7)	2.3938(17)	114.64	77.84	0.155
4a[e]	1.861(5)	2.203(1)	116.84	90.00	1.161
4b	1.874(3)	2.2055(8)	116.23	88.81	0.698
4c[e]	1.863(5)	2.2172(13)	115.04	83.46	0.228

[a] Angle between the mean square planes defined by *i)* the six atoms of the heterocycle (plane1) and *ii)* by the metal centre and the four atoms bound to the metal (plane2). [b] Distance of the metal-bound carbon atom from plane2 as a probe for the distortion of the square planar geometry. [c] Inaccurate, due to disorder of the ligand (*cf.* supporting information). [d] Ref. 20 [e] Ref. 21

As stated earlier,[18] examination of M-C distances is not a versatile tool to prove or rule out carbene-type bonding because differences are usually not significant. Similarly, hindered rotation about the M-C bond does not seem to reflect increased M-C bond order.[43]

On the other hand, the observed static *trans* influences seem to show a consistent trend: the further the heteroatom occurs from the carbene carbon atom, the longer the *trans* M-Cl bond becomes. Bond lengthening is accompanied by a decrease in the internal bond angle at the carbene carbon (CCX; X = N, C). However, the differences are small and might be influenced by intermolecular dipole-dipole interactions in the solid state.[44]

Bercaw and coworkers have discussed the bonding situation for *normal* pyridylidene complexes in terms of the bond alternation within the heterocyclic carbene ligand.[45] We followed a similar approach in our efforts to identify relevant contributing structures for the complexes **4** (Scheme 3).[46]

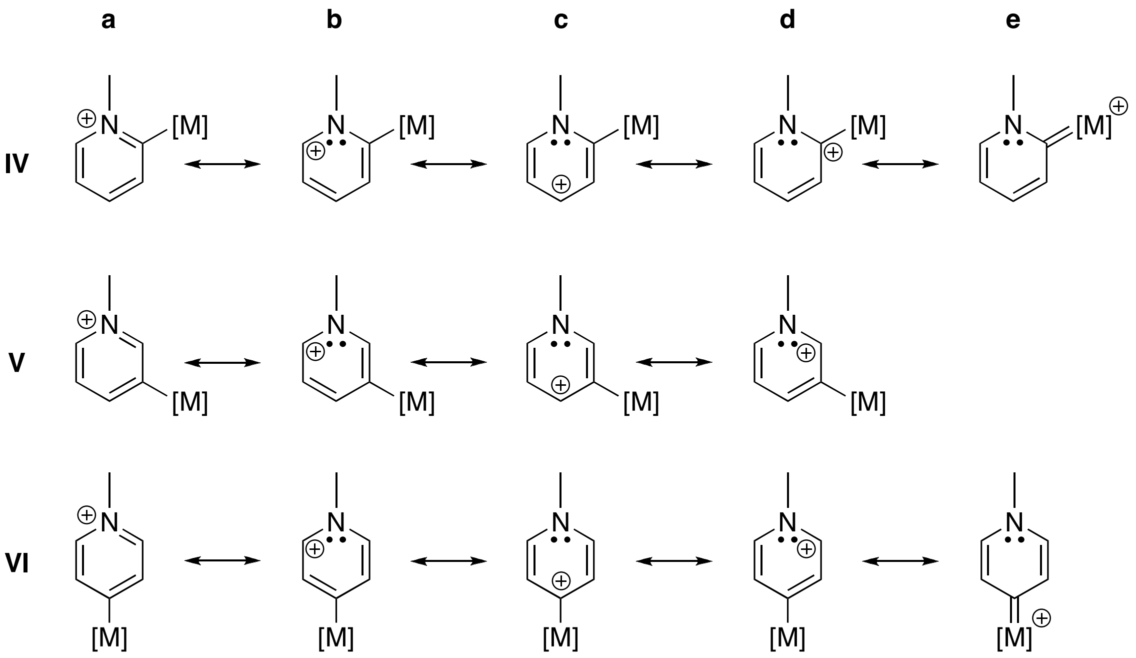

Scheme 3: Various mesomeric structures of *normal* (**IV**, **VI**) and *abnormal* (**V**) pyridylidene complexes - some of them *remote* (**V**, **VI**).

The 2-pyridylidene moiety in **4a** shows a significant increase in the N1-C6 and C2-C3 distances when compared to free pyridine (Figure 2). However, the N1-C2 bond remains short. These observations could indicate the relative importance of contributing structures like **IVa** and **IVe** in Scheme 3. A weak diene-type character of 2-pyridylidenes has been suggested earlier by others.[47] Remarkably, examination of available structural data on 2-pyridone reveals a rather similar bond distribution pattern therein (Figure 2).

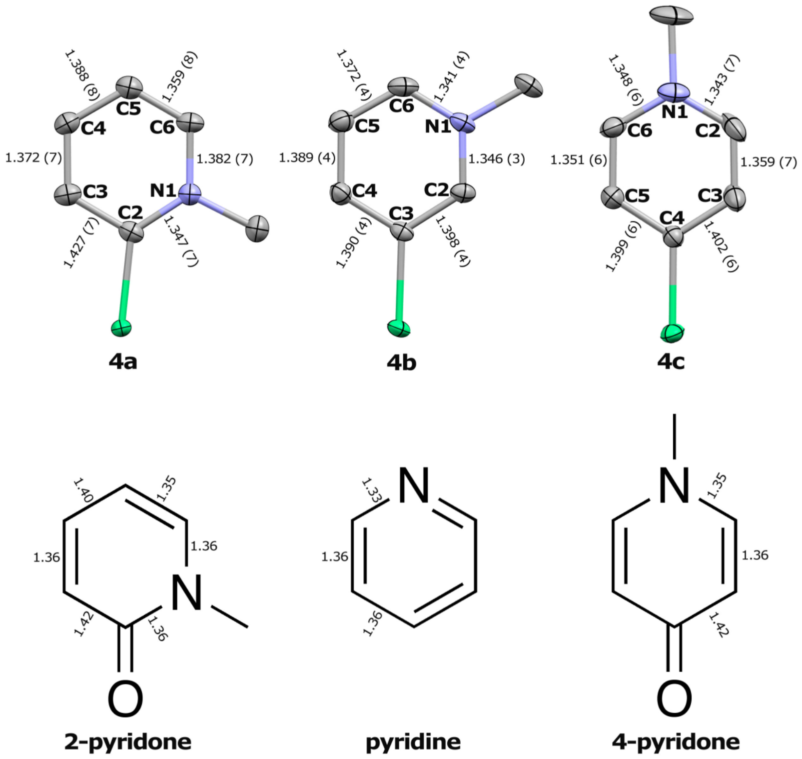

Figure 2: Bond distances (Å) in **4a**, **4b**, and **4c** (top) in comparison to those in free pyridine and pyridones (bottom - data derived from CCSD[48])

Evidence for a diene-like contribution such as **VIe** (Scheme 3), is also found in the 4-pyridylidene ligand of **4c**. The lateral bonds C2-C3 and C5-C6 are significantly (4.3σ) shorter than those of C3-C4 and C4-C5 (Figure 2). Related bond variations are also found for 4-pyridylidene tungsten[25] and platinum complexes.[31] The latter comprise a short Pt-C bond and a ^{13}C carbene resonance as high as 324 ppm. Again, a similar geometry is featured by the corresponding 4-pyridone.

In contrast to the heterocyclic rings of the two *normal* pyridylidene ligands in **4a** and **4c** where internal distances qualitatively support carbenoid mesomers (**IVe** and **VIe**, respectively), the *abnormal* bonding in complex **4b** entails bond length variations that cannot be readily described in terms of simple valence bond resonance theory. Nevertheless, consistent with the examples above, bonds that involve the nitrogen atom are relatively short (N1-C2, N1-C6), while bonds from the carbene carbon atom are rather long (C2-C3, C3-C4).

Such findings are particularly relevant when considering that the bond length variations found in complexes **4** are not observed in the corresponding chloropyridinium precursor salts (see supporting information for details). In contrast to the situation in the metal complexes, the atom separations are not significantly dependent on the substitution pattern, and are closely related to those in unsubstituted pyridinium salts. We therefore conclude that metallation, rather than alkylation, has the greatest influence on the bonding within the heterocyclic ligands during ylidene formation from chloropyridines. Furthermore, this influence of the metal fragment seems to be related to the effect that a doubly bound oxygen exerts in pyridones. These arguments all point towards a non-negligible double bond character of the metal carbon bonds in the *normal* pyridylidene complexes.

Interestingly, the *non-methylated* 4-pyridyl ligand in palladium complex **A** displays similar features to those of the pyridylidene ligand in **4c**, *i.e.* short lateral bonds.[49] It could be reasoned, that coordination to the metal centre already induces localization of double bonds in a carbenoid fashion (Figure 3 – **A'**). Indeed, according to electron decomposition analysis (EDA), σ and π orbital contributions in pyridyl-metal and pyridylidene-metal bonds are remarkably similar.[24] This result also provides an explanation for the increased basicity of the nitrogen in pyridyl metal complexes which can even lead to the activation of dichloromethane.[50-55]

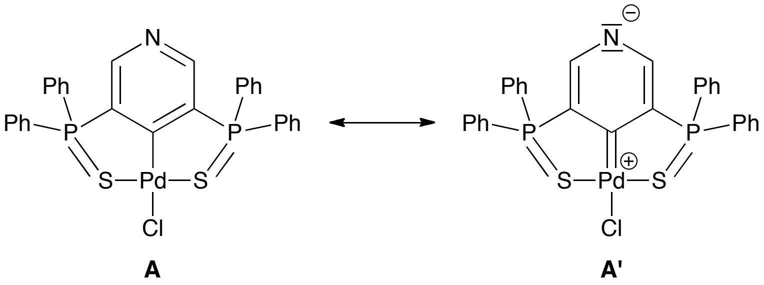

Figure 3: Metal-induced carbenoid electron distribution prior to formal carbene formation (*via* methylation or protonation)

c) NMR Spectroscopic Characterization

Similar to the difficulties experienced when attempting to determine "carbene character" from metal-carbene bond lengths, a comparison of absolute carbene carbon NMR shift values also does not give clear answers.[18] We have previously noted that correlation of NMR data with data of other analytical techniques, e.g. IR ν(CO) stretching frequencies, is often poor thus requiring cautious interpretation.[18] In the series of complexes **3** and **4**, significantly lower frequencies are observed for the *abnormal* complexes **3b** and **4b** (δ_C 165 and 174, respectively) than for the *normal* congeners ($\delta_C > 190$). When compared to the corresponding carbon resonances in the precursor pyridinium salts, deshielding between 30 and 50 ppm occurs upon formal carbene formation. For both metals, *abnormal* C3-bonding induces the smallest and *normal* remote C4-bonding the largest shift difference. Nickel bonding shows consistently a stronger deshielding effect than palladium coordination.

In order to correlate the structural investigations with solution properties, we also elucidated the electronic influence of alkylation and metallation on the heterocyclic ring by NMR spectroscopy. Comprehensive interpretation of the ^{1}H NMR chemical shifts is hampered by the phosphine signals in the aromatic region which overlap with the protons of the heterocyle. Hence, we concentrated on ^{13}C NMR data, which are known to be less affected by long-range magnetic and solvent effects,[56] and which correlate well with ^{1}H data in aromatic systems.[56,57] Figure 4 summarizes the most relevant chemical shifts.

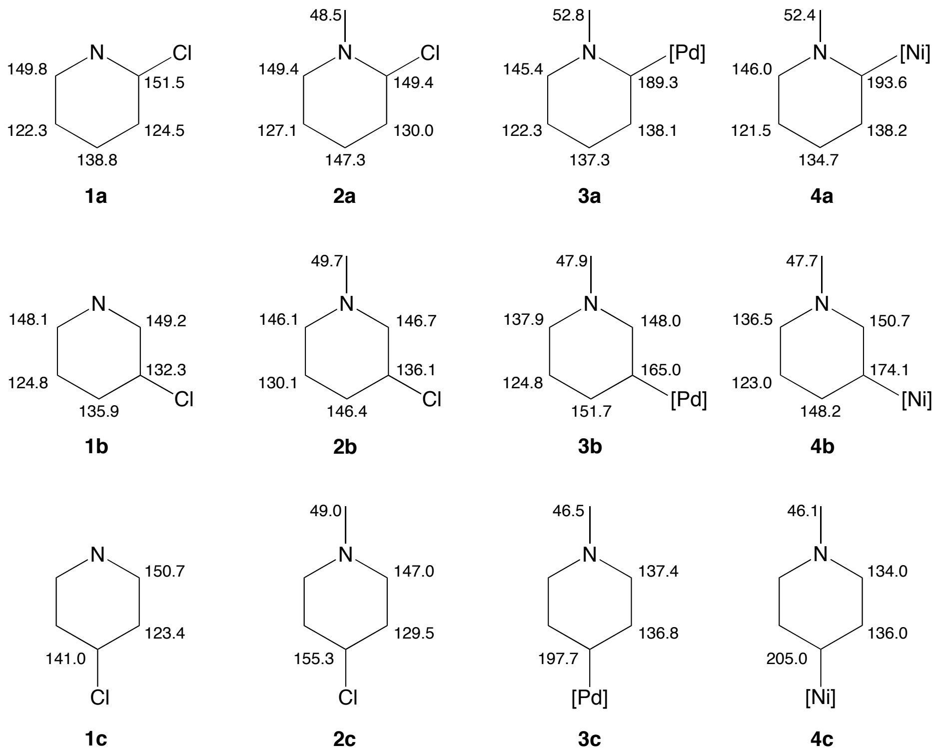

Figure 4. Summary of ^{13}C NMR chemical shifts in ppm

Linear correlations between the chemical shift and the charge density on a given atom in a homologous series of compounds are often used for the interpretation of NMR results.[58] Using calculated charge densities, such a dependence has been shown to exist for azine derivatives,[59] as well as for palladium pyridyl complexes.[60] The latter complexes, however, show a specific behaviour for the metal-bound carbons, which can be attributed to anisotropic effects.[61-63] In our series of compounds, linear regression of the calculated charges in **1a-c**[64] and experimental NMR measurements (Figure 4) also yields an appreciable fit ($R^2 = 0{,}91$ - see supporting information). We therefore assume that the ^{13}C NMR data of the heterocyclic carbons that are not bound to the metal offer a qualitative probe for the partial charge (re)distributions during complex formation. Information about relative charge densities at the nitrogen atom can be derived indirectly through the N-methyl carbon resonance.[65] Counterion effects may be insignificant since the triflate salts show negligible alteration of shifts when compared to the corresponding BF_4^- analogues, some of which have been reported earlier.[20,21]

Based on these considerations, nitrogen methylation of the chloropyridines **1a**-**c** affects mostly the region remote to the nitrogen atom. Evidently, the heteroatom – now with increased effective electronegativity – compensates for the loss of its lone pair by draining electron density from the ring and thus decreases the electron density especially at the 4-position significantly in the pyridinium salts **2** regardless of the chloro-substitution pattern. Even though the upfield shift for C2 and C6 is marginal, it might be attributed to a decrease in the N1-C2 and N1-C6 bond orders.[66]

Subsequent metal insertion at the 2-position of **2a** to form **3a** or **4a** induces a drift of the positive charge in the ring towards the vicinity of the metal thus indicating contributions from resonance structures **IVa**, **IVd** and **IVe** (*cf.* Scheme 3). Simultaneously, a secondary process apparently increases the electron density at the carbon atoms that are remote to the coordination site. Owing to this effect, the ^{13}C NMR chemical shifts of the neutral starting compound **1** are somewhat restored in the ligand backbone which is in agreement with predominant charge stabilization within the N-$C_{carbene}$-M moiety.

The importance of contributing structures similar to **VIc** and **VIe** (Scheme 3) for the *remote* 4-pyridylidene complexes **3c** and **4c** is reflected by a significant charge redistribution within the heterocycle upon carbene formation. Again, metal insertion effects deshielding of the carbon atoms adjacent to the metal-bound carbon and concurrent shielding of the remote nuclei. Even the nitrogen atom possibly becomes less positively charged as is shown by a small upfield shift for the attached methyl group. Due to the mutual *trans* arrangement of nitrogen and carbene carbon atoms, the polarization in the complex is sufficiently large to render the carbons in *ortho* and *meta* position almost magnetically equivalent. This result lends further support to the carbene character of C4-pyridylidene complexes (**VIe**, *cf.* X-ray discussion), and it is also in agreement with NBO analysis, which revealed that a Lewis structure resembling **IIIa** (Scheme 1) is most appropriately describing a *free* 4-pyridylidene.[67]

For *abnormal* C3-pyridylidene complexes, interpretation of the NMR results in terms of valence bond theory is not straightforward, thus paralleling the solid state conclusions. However, the ^{13}C NMR data indicate consistently for all pyridylidenes that metallation induces a deshielding effect in the vicinity of the metal combined with shielding of the remote heterocyclic nuclei. Similar observations have also been made by Isobe and coworkers[50] for neutral non-methylated bromopyridines upon insertion of $Pd(PEt_3)_2$ into the carbon-halide bond. This effect may thus be independent of the coordination mode of the ligand (*normal vs. abnormal*) or its partial charge (pyridylidene *vs*. pyridyl). Computational studies support such a conclusion, since the σ and π orbital contributions in pyridyl-metal and pyridylidene-metal bonds have been calculated to be remarkably similar.[24]

Consistent with our conclusions from crystallographic analyses, the observed influence of the metal fragment on the heterocycle might be rationalized by non-negligible $M \rightarrow L$ π-backdonation. In general, an essentially similar but stronger shielding/deshielding behaviour is observed for the nickel(II) fragment compared to palladium(II). This effect may tentatively be assigned to a larger M=C double bond character in **4** than in the corresponding palladium complexes **3**.

Singlets in the ^{31}P NMR spectra of all complexes indicate the equivalence of both phosphine ligands, hence confirming a mutual *trans* arrangement also in solution (Scheme 2). Even though the resonances for complexes **3** and **4** fall in a narrow range (δ_P 22.7–24.9 and 21.2–23.0, respectively), both series show a common trend, *i.e.* 2- < 4- < 3-pyridylidene, suggesting an increasing donor strength of the carbene ligand in this order.[68]

c) Computational Studies

Calculations for the series of isomeric palladium and nickel model complexes ***M*3** and ***M*4** comprising PH_3 ligands instead of PPh_3 were conducted at the BP86/TZ2P level of theory to verify and extend our interpretation of experimental results (Table 2). The calculated M-C bonds are slightly shorter than the experimental values while the theoretical M-Cl distances are a bit longer than the X-ray data but the differences are not very large. The very small changes in the M-C and M-Cl bond lengths are within the error range of the theoretical and experimental data and thus, they do not exhibit a noticeable trend. The theoretical and experimental CCX bond angles agree well. Also bond length variations within the rings, which were discussed in section b), are qualitatively reproduced. The calculated data of the model compounds may thus be used for the interpretation of the experimental findings.

Table 2. Computational results at the BP86/TZ2P level and comparison with experimental values which are given in *in italics*.

	d(M-C) [Å]	**d (M-Cl) [Å]**	**CCX angle [°]**	**E_{rel} [b] [kcal mol^{-1}]**	**E_{int} [c] [kcal mol^{-1}]**
***M*3a**	2.021	2.342	116.23	0	-95.9
	2.002(3)	*2.3638(8)*	*116.22*		
***M*3b**	2.029	2.347	115.67	3.25	-105.9
	1.996(7)	*2.371(2)*	*117.82*		
***M*3c**	2.019	2.339	115.34	3.47	-109.3
	1.979(7)	*2.3938(17)*	*114.64*		
***M*4a**	1.873	2.189	116.10	0	-101.6
	1.861(5)	*2.203(1)*	*116.84*		
***M*4b**	1.881	2.192	115.47	3.61	-111.3
	1.874(3)	*2.2055(8)*	*116.23*		
***M*4c**	1.877	2.179	115.13	3.72	-115.5
	1.863(5)	*2.2172(13)*	*115.04*		

[a] Compared to experimental values (*cf.* Table 1). [b] Relative minimized energies. [c] metal-carbene interaction energies.

The relative energies of the model systems ***M*3** and ***M*4** follow the trend 2-pyridylidene << 3-pyridylidene < 4-pyridylidene which is the same order that has been reported for the corresponding *free* carbene isomers of pyridine, in which one proton is located on the nitrogen atom.[24,27,28] However, the energy differences are much smaller in the complexes which can be rationalized by the calculated stronger interactions in 3- and 4-pyridylidene complexes which partly compensate the energy difference in the free pyridylidenes. The energy decomposition analysis of the metal-carbon bonds reveals increasing interaction energies (E_{int}) in the order 2-pyridylidene < 3-pyridylidene < 4-pyridylidene . In an extensive EDA study of pyridylidene and quinolylidene M-C bonds we could show that E_{int} correlates very well with the energy of the HOMO, *i.e.* the σ lone-pair orbital of the carbene and thus the σ donor properties of a given ligand.[24]

e) Catalysis

In order to determine the influence of abnormal and remote pyridylidene bonding modes on catalytic performance, the palladium complexes **3** were used in Suzuki-Miyaura cross-coupling reactions (Scheme 4).[69] Results of preliminary experiments under standard conditions indicated small but distinct differences in the catalytic activity. As a general trend, increasing remoteness enhanced the conversions, and yields of the biaryl product followed the trend **3c** (86%) > **3b** (82%) > **3a** (78%). All complexes displayed better performance than the reference complex $Pd(PPh_3)_4$ (71%). The trend was slightly more pronounced when using milder reaction temperatures and working under an inert atmosphere (Figure 5 - also see supporting informations).

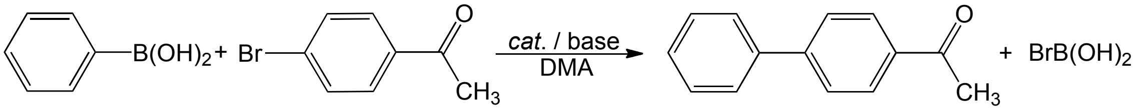

Scheme 4: Suzuki-Miyaura-type test reactions.

No palladium black was observed during catalysis, thus suggesting a homogeneous mode of action. This assumption is further supported by the pertinent time-conversion profiles, which do not show any induction time or sigmoidal substrate conversion. Time-dependent monitoring also unveiled further subtle differences between the pyridylidene-based catalytic systems (Figure 5). The initial catalytic activity during the first two hours is very similar for all three complexes, perhaps slightly higher for the normal carbene complex **3a**. However, this complex seems to be the least robust and deactivates after extended periods of reaction time, thus not reaching high conversions. In contrast, the remote pyridylidene complexes **3b** and **3c** remain active even after 20 hours of activity. Hence the general trend stated above need to be refined. While the *normal* pyridylidene complexes **3a** and **3c** are slightly more active than *abnormal* **3b**, the *remote* complexes **3c** and **3b** are more robust than **3a**. Since the differences observed here are only small, further tests will be needed in order to substantiate the deduced trends.

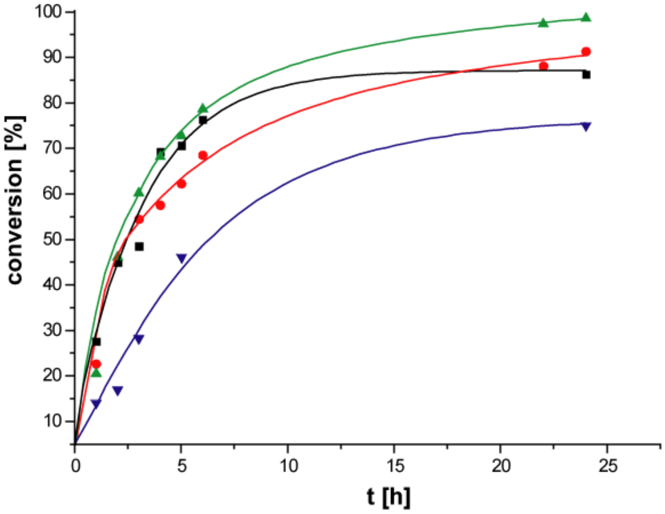

Figure 5. Time/conversion curves under inert conditions (**3a** squares; **3b** dots; **3c** triangles; $Pd(PPh_3)_4$ inverted triangles).

f) Regioselectivity of the Oxidative Addition of Pyridylium Salts

In addition to comparing the possible bonding modes of pyridylidenes, we were also interested to determine how carbene formation would preferentially occur when the metal complex reactant was presented with two active Cl-containing sites on the pyridinium ring. Reactions of $M(PPh_3)_4$ (M = Pd, Ni) with the dichlorinated methyl-pyridinium salt **5** in toluene (Scheme 5) yielded, according to ^{13}C and ^{1}H NMR, exclusively the 4-pyridylidene complexes **6** and **7**. In comparison with the unsubstituted analogue **3c**, complexes **6** shows a ca. 5 ppm downfield shift of the carbene resonance, which can be attributed to the *meta*-influence of the chloride substituent. The ^{31}P signals differ only insignificantly.

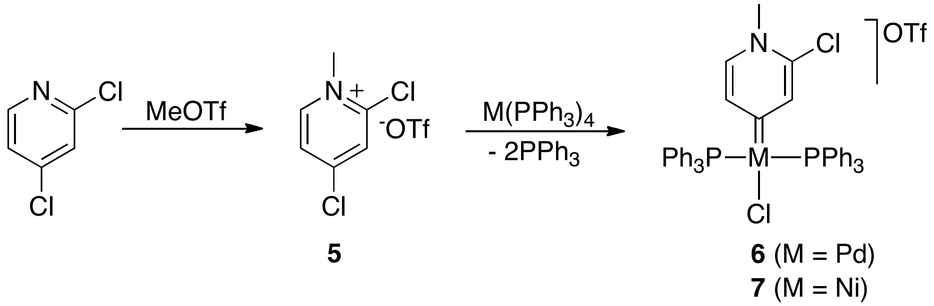

5

Scheme 5: Oxidative addition in a competitive environment yields exclusively the 4-pyridylidene complexes **6** and **7**.

X-ray crystal structure determinations of **6** and **7** unambiguously confirmed the coordination sites deduced by NMR spectroscopy (Figure 6). The observed features are generally similar to those discussed above. Notably, the M-C distances of 1.972(4) and 1.855(2) Å for **6** and **7**, respectively, both represent the shortest bonds in the series of pyridylidene complexes discussed in this article. The M-Cl bonds are within the range described.

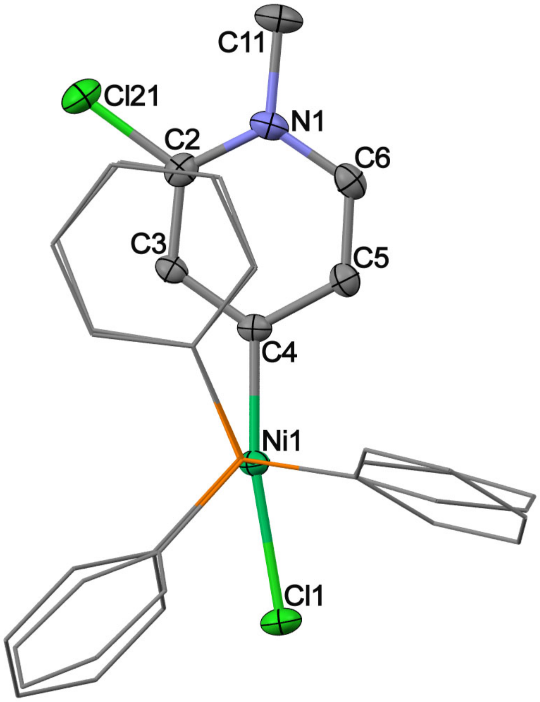

Figure 6: Molecular structure of **7** (50% probability ellipsoids, hydrogen atoms and counterion omitted). Selected bond lengths [Å] and angles [°]: Ni1-C4 1.855(2), N1-C2

1.356(3), C2-C3 1.372(3), C3-C4 1.399(3), C4-C5 1.410(3), C5-C6 1.1359(3), C6-N1 1.355(3); C3-C4-C5 116.6(2), C4-Ni1-Cl1 170.24(7).

Based on the steric shielding effect of the N-methyl group in **5** and with reference to the seminal work by Carmona and coworkers,[33,34,47] the observed regioselectivity of metallation might be ascribed to steric discrimination. However, the same selectivity was observed when the protonated analogue of **5** was used as ligand precursor. While the palladium homologue of **6** could not be obtained in pure form, NMR spectra clearly indicated the formation of the C4-bound complex as the main product and the only carbene species (for details see experimental section). A good agreement with the signals in the spectra of **6** and especially $^2J_{CP}$ couplings for two carbon atoms are indicative for the selective formation of the C4-bound isomer. Obviously, metallation of the remote 4-position is not sterically triggered but is electronically preferred.

The fact that metal attack occurs preferentially at the remote position can be understood against the background of established pyridine cross-coupling chemistry.[70] Although the aryl addition mechanism in such reactions is still a matter of debate, all proposed pathways (*i.e.* concerted, S_N2, free halide)[71-73] feature the electron-rich d^{10} metal as a nucleophile. Accordingly, preferential attack at the most electron-deficient 2-position can be assumed and is indeed observed. For example 2,4-dibromopyridine is metallated by $Pd(PPh_3)$ almost exclusively in the *ortho*-position.[74] This corresponds to the most deshielded carbon atom according to NMR results (C2: δ_C 142.5; C4: δ_C 133.9). In our case, where the precursor **5** features ^{13}C carbon shifts of 148.9 and 156.0 ppm for C2 and C4, respectively, attack also occurs at the most deshielded (*i.e.* the presumably more electrophilic) site.

Calculation of the relative energies for realistic models of **6** and **7** (Figure 7) at the BP86/TZVPP level of theory, revealed that the 2-pyridylidene complexes ***M6'*** and ***M*7'** are more stable than the 4-congeners ***M*6** and ***M*7** (E_{rel} in Table 3). The same trend was calculated for the 2- and 4-substituted isomers **M3a**/**M3c** and **M4a**/**M4c** (Table 2) which suggests that the relative stability of the 2- and 4-substituted systems does not depend on the steric requirements of the ligand. We also calculated the computationally less demanding 4-substituted model compounds ***M*8**/***M*9** and their 2-substituted congeners ***M*8'**/***M*9'** and found a similar energy difference in favor of the latter isomers as for the bulkier compounds (Table 3). Energy decomposition analysis (EDA) on these simpler models further shows that the stronger interaction occurs in the *para* position (E_{int} in Table 3). These findings are consistent with the results shown in Table 2 and with our previous EDA studies on pyridylidenes.[24]

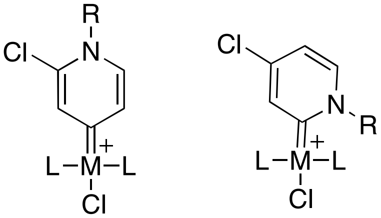

***M*6** ***M*6'** (M = Pd; L = PPh_3; R = Me)
***M*7** ***M*7'** (M = Ni; L = PPh_3; R = Me)
***M*8** ***M*8'** (M = Pd; L = PH_3; R = H)
***M*9** ***M*9'** (M = Ni; L = PH_3; R = H)

Figure 7: Models of the possible products formed upon oxidative addition in Scheme 5.

Table 3. Computational results.

	E_{rel} [a] [kcal/mol]	E_{int} [b] [kcal/mol]
***M*6** [c]	7.9	n/a
***M*6'** [c]	0	n/a
***M*7** [c]	6.9	n/a
***M*7'** [c]	0	n/a
***M*8** [d]	5.6	-103.1
***M*8'** [d]	0	-91.0
***M*9** [d]	4.9	-109.3
***M*9'** [d]	0	-96.6

[a] Relative minimized energies. [b] Bond interaction energies. [c] BP86/TZVPP. [d] BP86/TZ2P.

The theoretically predicted higher stability of the 2-pyridylidene complexes ***M6'*** and ***M7'*** and the experimental finding that only the 4-congeners **6** and **7** are found indicate that the less stable isomers are the product of a kinetically controlled reaction. This is a very important result which we shall investigate in a future study. We do not think that the calculations predict a wrong stability order, because we obtain the same trend with similar energy differences using different methods. Also, since the calculations involve different isomers of the same molecule it can be expected that the results are quite reliable. A theoretical study of the reaction course is quite expensive because different pathways are possible. The theoretical work shall therefore be complemented by kinetic studies.

As an extension of our studies on quinolylidenes,[20,21,23,40-42] we also compared the reactivity of $M(PPh_3)_4$ towards dichloroquinolinium salts **8** where both chloro substituents (Scheme 6) are three bonds removed from the methylated (R = Me) or protonated (R = H) nitrogen atom. Again, only one of the possible products was formed in each reaction. Consistent with the expected electrophilicity derived from the ^{13}C NMR spectra of the precursors, (C4: δ_C 155; C7: δ_C 144), metallation is preferred within the N-containing ring to yield complexes **9** and **10**. In comparison with the monocyclic congeners in **3c** and **4c**, the quinolylidene carbene signals are shifted about 10 ppm downfield while the ^{31}P NMR shifts remain essentially identical.

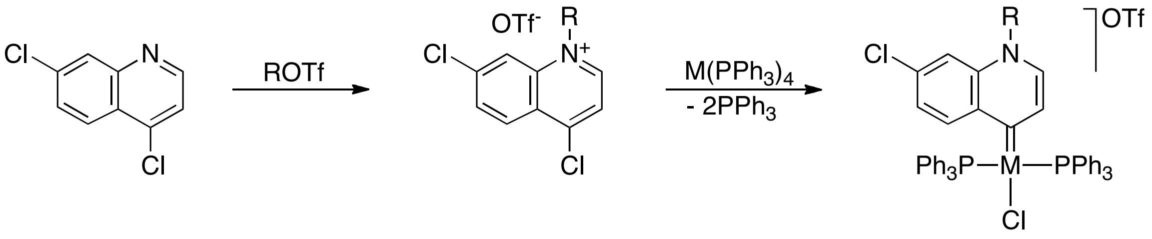

8a (R = Me)
b (R = H)

9 (M = Pd)
10 (M = Ni)

Scheme 6: Competitive oxidative addition at dichloroquinolinium salts.

No traces of any dinuclear complexes were found even when using an excess of metal precursor. Figure 8 depicts the crystal structure of **9a**, indicating that the presence of bulky phosphine ligands excludes the formation of dinuclear products.

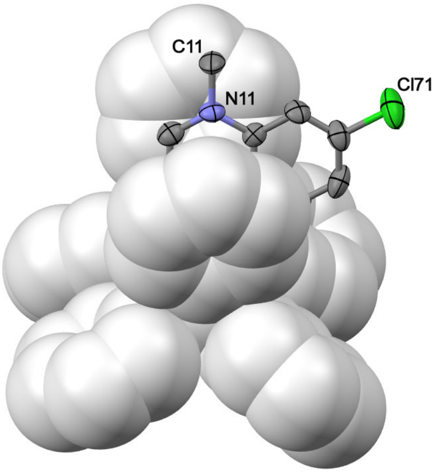

Figure 8: Occlusion of the quinolylidene ligand by PPh_3 ligands in **9a**.

Conclusions

While X-ray structural data and ^{13}C NMR measurements of the *normal* (both adjacent and *remote* to N) complexes within a complete set of pyridine-derived carbene complexes consistently support a carbenoid-type bonding (*i.e.* partial M=C double bond character), results for the *abnormal* examples cannot be described in terms of simple valence bond resonance theory. Close examination reveals a coherent and consistent influence of the metal fragments on the heterocyclic ligand in all bonding modes. Due to an apparent influence of *remote* carbene bonding on catalytic robustness, this concept seems slightly more relevant for catalytic application than the variation between *normal* and *abnormal* bonding situations. In an investigation of competitive carbene complex formation by oxidative insertion, *remote* 4-pyridylidene formation is favoured over that of 2-pyridylidene formation even in the absence of steric shielding at nitrogen. Overall, we conclude that the concepts of *remote* and *(ab)normal* carbene bonding are useful and their differences well reflected in our experimental observations in various pyridylidene complexes of Pd and Ni.

Experimental Section

General

All manipulations were performed in a dry argon atmosphere using standard Schlenk techniques. $Pd(PPh_3)_4$[75] was prepared using a previously published method. All other chemicals were commercially available. Diethyl ether, hexane and pentane were freshly distilled under N_2 from sodium wire and CH_2Cl_2 from CaH_2. Melting points (uncorrected) were determined on a Stuart SMP3 apparatus. NMR spectra were determined on a Varian 300 FT or INOVA 600MHz spectrometer (^1H NMR at 300/600 MHz, $^{13}C\{^1H\}$ NMR at 75/151 MHz and $^{31}P\{^1H\}$ NMR at 121.5/243 MHz). ^1H and ^{13}C chemical shifts refer to $\delta_{TMS} = 0.00$ according to the residual deuterated solvents and are reported in ppm. ^{31}P chemical shifts are reported in ppm relative to an 85% H_3PO_4 external standard. FAB-MS determinations were performed on a VG 70SEQ mass spectrometer in a 2-nitro benzyl alcohol matrix at the University of Witwatersrand, South Africa.

Procedure A: preparation of methylated triflate salts.

A small excess (1.1 molar equivalents) of methyl trifluoromethanesulfonate was added dropwise to a solution of the respective pyridine/quinoline precursor in 20 ml of CH_2Cl_2. The solution was stirred for 18 hours at room temperature where after the solvent was removed by cannula. The resulting precipitate was washed with ether (3 x 10 ml) and dried under high vacuum for a few hours.

For the synthesis of the 4-substituted salt, 4-chloropyridine·HCl (5.00 g, 33.3 mmol) was dissolved in 50 ml of distilled water and 40 ml 1 M NaOH was added. The aqueous solution was extracted with ether (3 x 40 ml). The organic phase was washed with brine, dried with $MgSO_4$ and concentrated in a brown Schlenk tube. The oil (2.18 g, 19.2 mmol) was dissolved in CH_2Cl_2, cooled to -78 °C and methyl trifluoromethanesulfonate (3.46 g, 2.40 ml, 21.1 mmol) was added drop wise. The mixture was stirred overnight while it was allowed to warm up to room temperature. The solvent was removed *in vacuo* and the resulting product was washed once with 10 ml of THF and twice with 10 ml of diethyl ether.

Procedure B: preparation of protonated triflate salts.

The hydropyridinium triflate salts were obtained by reacting the ligand precursor with a small excess (1.1 molar equivalents) of CF_3SO_3H in 20 ml of CH_2Cl_2 at room temperature for 18 hours. Diethyl ether (20 ml) was added and a white precipitate formed. The solvent was removed *via* a cannula and the resulting solid washed with 4 x 20 ml diethyl ether and dried *in vacuo*.

Procedure C: Preparation of *trans*-Chloro(pyridylidene)bis(triphenylphosphine)-palladium(II) triflate complexes.

The respective triflate salts and a small excess (1.01 molar equivalents) of $Pd(PPh_3)_4$ were suspended in 30 ml of toluene and stirred for 17 hours at 60 °C (in the case of **3b**, the reaction mixture was stirred for 64 hours). The white suspension in a light yellow solution was allowed to cool to room temperature and filtered through celite. The solid on the filter was washed with 4 x 5ml toluene and the product was dissolved in CH_2Cl_2 and filtered, to yield after solvent evaporation *in vacuo* the microcrytalline palladium complexes.

Procedure D: preparation of *trans*-Chloro(pyridylidene)bis(triphenylphosphine)-nickel(II) triflate complexes.

A small excess (1.1 molar equivalents) of $Ni(PPh_3)_4$ and the respective triflate salt were suspended in THF (20 ml) and the mixture was stirred at room temperature for 17 hours. The resulting yellow precipitate in a brown solution was filtered through celite was washed with 3 x 5 ml toluene. The product was dissolved in CH_2Cl_2, filtered and dried under high vacuum.

2-chloro-1-methylpyridinium triflate, 2a.

According to procedure A: 88.0 % yield of colourless micro-crystalline material; m.p.: 163.3 – 165.0 °C. ^1H NMR (CD_2Cl_2, 20°C): $\delta = 4.49$ (3H, s, NMe), 8.02 (1H, m, H^5), 8.06 (1H, dd, ^{3}J = 8.3 Hz, ^{4}J = 1.3 Hz, H^3), 8.45 (1H, td, ^{3}J = 8.3 Hz, ^{3}J = 1.7 Hz, H^4), 9.18 (1H, dd, ^{3}J = 6.2 Hz, ^{3}J = 1.7 Hz, H^6). ^{13}C {^{1}H} NMR (CD_2Cl_2, 20°C): δ = 48.5 (s, NMe), 127.1 (s, C^5), 130.0 (s, C^3), 147.3 (s, C^4), 149.4 (bs, C^2 and C^6), CF_3 not observed. Anal. Calc. for $C_7H_7NO_3SClF_3$ (277.65 g·mol^{-1}): C 30.28, H 2.54, N 5.04 Found: C 30.01, H 2.41, N 4.93.

3-chloro-1-methylpyridinium triflate, 2b.

According to procedure A: 98.5 % yield of colourless micro-crystalline material; m.p.: 60.8 – 62.3 °C. ^{1}H NMR (CD_2Cl_2, 20°C): δ = 4.63 (3H, s, NMe), 8.29 (1H, dd, ^{3}J = 8.3 Hz, ^{3}J = 6.3 Hz, H^5), 8.81 (1H, dm, ^{3}J = 8.3 Hz, ^{4}J = 0.5 Hz, H^6), 9.15 (1H, d, ^{3}J = 6.3 Hz, H^4), 9.38 (1H, d, ^{4}J = 0.5 Hz, H^2). ^{13}C {^{1}H} NMR (CD_2Cl_2, 20°C): δ = 49.7 (s, NMe), 130.1 (s, C^5), 136.1 (s, C^3), 146.1 (s, C^6), 146.4 (s, C^4), 146.7 (s, C^2), CF_3 not observed. MS (FAB): *m/z* (%) = 130.1 (35) $[M-CF_3SO_3]^+$, (^{37}Cl); 128.1 (100) $[M-CF_3SO_3]^+$, (^{35}Cl). Anal. Calc. for $C_7H_7NO_3SClF_3$ (277.65 g·mol^{-1}): C 30.28, H 2.54, N 5.04 Found: C 30.80, H 2.30, N 5.09.

4-chloro-1-methylpyridinium triflate, 2c.

According to procedure A: 55.5 % yield of colourless micro-crystalline material; m.p.: 135.1 – 136.6 °C. ^{1}H NMR (CD_2Cl_2, 20°C): δ = 4.45 (3H, s, NMe), 8.01 (2H, d, ^{3}J = 6.8 Hz, H^3 and H^5), 8.82 (2H, d, ^{3}J = 6.8 Hz, H^2 and H^6). ^{13}C {^{1}H} NMR (CD_2Cl_2, 20°C): δ = 49.0 (s, NMe), 129.5 (s, C^3 and C^5), 147.0 (bs, C^2 and C^6), 155.3 (s, C^4), CF_3 not observed. Anal. Calc. for $C_7H_7NO_3SClF_3$ (277.65 g·mol^{-1}): C 30.28, H 2.54, N 5.04 Found: C 30.01, H 2.61, N 5.11.

***trans*-Chloro(2-hydro-1-methyl-2-pyridylidene)-bis(triphenylphosphine)-palladium(II) triflate, 3a.**

According to procedure C: 96.3 % yield of colourless micro-crystalline material; m.p.(dec.): 248 °C. ^{1}H NMR (CD_2Cl_2, 20°C): δ = 3.96 (3H,s, NMe), 7.00 (2H, m, H^4 and H^5), 7.40, 7.52 (31H, m, PPh with obscured H^6), 7.89 (1H, d, ^{3}J = 6.0 Hz, H^3). ^{13}C {^{1}H} NMR (CD_2Cl_2, 20°C): δ = 52.8 (s, NMe), 122.3 (s, C^5), 128.9 (m, PPh^{ipso}), 129.3 (m, PPh^{meta}), 131.8 (s, PPh^{para}), 134.3 (m, PPh^{ortho}), 137.3 (s, C^4), 138.1 (t, $^3J_{C\text{-}P}$ = 3.9 Hz, C^3), 145.4 (s, C^6), 189.3 (t, $^2J_{C-P}$ = 6.5 Hz, C^2), CF_3 not observed. ^{31}P {^1H} NMR (CD_2Cl_2, 20°C): δ = 22.7 (s, PPh_3). Anal. Calc. for $C_{43}H_{37}NO_3P_2SClF_3Pd$ (908.64 g·mol^{-1}): C 56.84, H 4.10, N 1.54. Found: C 57.03, H 4.19, N 1.60.

trans-Chloro(3-hydro-1-methyl-3-pyridylidene)-bis(triphenylphosphine)palladium(II) triflate, 3b.

According to procedure C: 90.8 % yield of colourless crystals; m.p.(dec.): 195 °C. Single crystals suitable for structure determination by were obtained by dissolving the crude mixture in CH_2Cl_2 and allowing pentane to diffuse slowly into the mixture at -20 °C.

^1H NMR (CD_2Cl_2, 20°C): δ = 3.54 (3H, s, NMe), 6.73 (1H, dd, ^3J = 7.7 Hz, ^3J = 6.0 Hz, H^5), 7.26 (1H, bs, H^2), 7.40, 7.49, 7.58 (30H, m, PPh), 7.78 (1H, d, ^3J = 7.7 Hz, H^4), 7.82 (1H, d, ^3J = 6.0 Hz, H^6). ^{13}C {^1H} NMR (CD_2Cl_2, 20°C): δ = 47.9 (s, NMe), 124.8 (s, C^5), 129.0 (m, PPh^{ipso}), 129.4 (m, PPh^{meta}), 131.4 (s, PPh^{para}), 134.8 (m, PPh^{ortho}), 137.9 (s, C^6), 148.0 (t, $^3J_{CP}$ = 4.9 Hz, C^2), 151.7 (t, $^3J_{CP}$ = 3.5 Hz, C^4), 165.0 (t, $^2J_{CP}$ = 6.9 Hz, C^3), CF_3 not observed. ^{31}P {^1H} NMR (CD_2Cl_2, 20°C): δ = 24.9 (s, PPh_3). MS (FAB): *m/z* (%) = 759.6 (52) $[M-CF_3SO_3]^+$, (^{35}Cl, ^{106}Pd); 498.0 (66) $[M-PPh_3-CF_3SO_3]^+$; 460.1 (21) $[M-PPh_3-Cl-CF_3SO_3]^+$; 384.7 (10) $[M-2PPh_3-Cl-CF_3SO_3]^+$. Anal. Calc. for $C_{43}H_{37}NO_3P_2SClF_3Pd$ (908.64 g·mol^{-1}): C 56.84, H 4.10, N 1.54. Found: C 56.99, H 4.01, N 1.60.

trans-Chloro(4-hydro-1-methyl-4-pyridylidene)-bis(triphenylphosphine)palladium(II) triflate, 3c.

According to procedure C: 99 % yield of colourless micro-crystalline material; m.p.(dec.): 189 °C. ^1H NMR (CD_2Cl_2, 20°C): δ = 3.80 (3H, s, NMe), 7.16 (2H, d, ^3J = 6.4 Hz, H^2 and H^6), 7.39 (14H, m, PPh with obscured H^3 and H^5), 7.50, 7.62 (18H, m, PPh). ^{13}C {^1H} NMR (CD_2Cl_2, 20°C): δ = 46.5 (s, NMe), 129.2 (m, PPh^{meta}), 130.0 (m, PPh^{ipso}), 131.7 (s, PPh^{para}), 135.2 (m, PPh^{ortho}), 136.8 (bs, C^3 and C^5), 137.4 (s, C^2 and C^6), 197.7 (t, ^2J = 6.5 Hz, C^4), CF_3 not observed. ^{31}P {^1H} NMR (CD_2Cl_2, 20°C): δ = 23.6 (s, PPh_3). Anal. Calc. for $C_{43}H_{37}NO_3P_2SClF_3Pd$ (908.64 g·mol^{-1}): C 56.84, H 4.10, N 1.54. Found: C 56.61, H 3.98, N 1.59

trans-Chloro(2-hydro-1-methyl-2-pyridylidene)bis(triphenylphosphine)nickel(II) triflate, 4a.

According to procedure D: 58.9 % yield of yellow micro-crystalline material; m.p.(dec.): 187 °C. ^{1}H NMR (CD_2Cl_2, 20°C): δ = 4.22 (3H, s, NMe), 6.81 (1H, m, H^5), 6.91 (1H, td, ^3J = 7.7 Hz, ^4J = 1.4 Hz, H^4), 7.42, 7.57 (31H, m, PPh with obscured H^6), 7.85 (1H, m, H^3). ^{13}C {^{1}H} NMR (CD_2Cl_2, 20°C): δ = 52.4 (s, NMe), 121.5 (s, C^5), 128.9 (m, PPh^{ipso}), 129.4 (m, PPh^{meta}), 131.8 (s, PPh^{para}), 134.5 (m, PPh^{ortho}), 134.7 (s, C^4), 138.2 (bs, C^3), 146.0 (s, C^6), 193.6 (t, $^3J_{CP}$ = 33.0 Hz, C^2), CF_3 not observed. ^{31}P {^{1}H} NMR (CD_2Cl_2, 20°C): δ = 21.2 (s, PPh_3). Anal. Calc. for $C_{43}H_{37}NO_3P_2SClF_3Ni$ (860.91 g·mol^{-1}): C 59.99, H 4.33, N 1.63. Found: C 60.32, H 4.24, N 1.49.

trans-Chloro(3-hydro-1-methyl-3-pyridylidene)bis(triphenylphosphine)nickel(II) triflate, 4b.

According to procedure D: 49.6 % yield of light yellow crystals; m.p.(dec.): 135.0 – 138.0 °C. Yellow crystals, suitable for single crystal X-ray structure determination, were obtained by slow diffusion of pentane into a concentrated CH_2Cl_2 solution at -20°C. ^{1}H NMR (CD_2Cl_2, 20°C): δ = 3.36 (3H, s, NMe), 6.69 (1H, m, H^5), 7.11 (1H, bs, H^4), 7.40, 7.66 (31H, m, PPh with obscured H^6), 8.09 (1H, d, ^4J = 4.4 Hz, H^2). ^{13}C {^{1}H} NMR (CD_2Cl_2, 20°C): δ = 47.7 (s, NMe), 123.0 (s, C^5), 128.9 (m, PPh^{meta}), 129.7 (m, PPh^{ipso}), 131.2 (s, PPh^{para}), 134.7 (m, PPh^{ortho}), 136.5 (s, C^6), 148.2 (s, C^4), 150.7 (bs, C^2), 174.1 (bs, C^3), CF_3 not observed. ^{31}P {^{1}H} NMR (CD_2Cl_2, 20°C): δ = 23.0 (s, PPh_3). MS (FAB): *m/z* (%) = 711.8 (8) $[M-CF_3SO_3]^+$, (^{37}Cl, ^{58}Ni); 449.6 (70) $[M-PPh_3-CF_3SO_3]^+$; 413.0 (24) $[M-PPh_3-Cl-CF_3SO_3]^+$. Anal. Calc. for $C_{43}H_{37}NO_3P_2SClF_3Ni$ (860.91 g·mol^{-1}): C 59.99, H 4.33, N 1.63. Found: C 60.21; H 4.20; N 1.73.

trans-Chloro(4-hydro-1-methyl-4-pyridylidene)bis(triphenylphosphine)nickel(II) triflate, 4c.

According to procedure D: 45.7 % yield of yellow micro-crystalline material; m.p.(dec.): 153 °C. ^{1}H NMR (CD_2Cl_2, 20°C): δ = 3.70 (3H, s, NMe), 6.91 (2H, d, ^3J = 5.9 Hz, H^2 and H^6), 7.40, 7.49, 7.68 (32H, m, PPh with obscured H^3 and H^5). ^{13}C {^{1}H} NMR (CD_2Cl_2, 20°C): δ = 46.1 (s, NMe), 128.8 (m, PPh^{meta}), 129.7 (m, PPh^{ipso}), 131.2 (s, PPh^{para}), 134.0 (s, C^2 and C^6), 134.7 (m, PPh^{ortho}), 136.0 (bs, C^3 and C^5), 205.0 (t, ^3J = 31.2 Hz, C^4), CF_3 not observed. ^{31}P {^1H} NMR (CD_2Cl_2, 20°C): δ = 22.4 (s, PPh_3). Anal. Calc. for $C_{43}H_{37}NO_3P_2SClF_3Ni$ (860.91 g·mol^{-1}): C 59.99, H 4.33, N 1.63. Found: C 60.21, H 4.23, N 1.54.

2,4-dichloro-1-methylpyridinium triflate, 5.

According to procedure A: 99.8 % yield of colourless micro-crystalline material; m.p.: 95.8 – 97.7 °C. ^1H NMR (CD_2Cl_2, 20°C): δ = 4.42 (3H, s, NMe), 7.99 (1H, dd, ^3J = 6.8 Hz, ^4J = 2.3 Hz, H^5), 8.05 (1H, d, ^4J = 2.3 Hz, H^3), 9.14 (1H, dd, ^3J = 6.8 Hz, ^5J = 0.4 Hz, H^6). ^{13}C {^1H} NMR (CD_2Cl_2, 20°C): δ = 48.1 (s, NMe), 127.7 (s, C^5), 130.1 (s, C^3), 148.9 (s, C^4), 150.0 (s, C^6), 156.0 (s, C^2), CF_3 not observed. MS (FAB): *m/z* (%) = 163.0 (77) $[M\text{-}CF_3SO_3]^+$, (^{37}Cl); 161.9 (100) $[M\text{-}CF_3SO_3]^+$, (^{35}Cl). Anal. Calc. for $C_7H_6NO_3SCl_2F_3$ (312.09 g·mol^{-1}): C 26.94, H 1.94, N 4.49 Found: C 26.88, H 1.99, N 4.57.

2,4-dichloro-1-hydropyridinium triflate.

According to procedure B: 85.7 % yield of colourless hygroscopic micro-crystalline material; m.p.: 115.4 – 117.0 °C. ^1H NMR (CD_2Cl_2, 20°C): δ = 7.94 (2H, m, H^3 and H^5), 8.79 (1H, m, H^6), NH not observed. ^{13}C {^1H} NMR (CD_2Cl_2, 20°C): δ = 126.8 (s, C^5), 128.7 (s, C^3), 144.7 (s, C^6), 146.6 (s, C^2), 157.0 (s, C^4), CF_3 not observed. MS (FAB): *m/z* (%) = 147.9 (100) $[M\text{-}CF_3SO_3]^+$, (^{35}Cl). Anal. Calc. for $C_6H_4NO_3SCl_2F_3$ (298.07 g·mol^{-1}): C 24.18, H 1.35, N 4.70. Found: C 23.29, H 1.41, N 4.54.

***trans*-Chloro(2-chloro-4-hydro-1-methyl-4-pyridylidene)-bis(triphenylphosphine)palladium(II) triflate, 6.**

According to procedure C: 74.3 % yield of colourless crystals; m.p.(dec.): 200 °C. ^1H NMR (CD_2Cl_2, 20°C): δ = 3.82 (3H, s, NMe), 7.16 (1H, bs, H^3), 7.41 (12H, m, PPh^{meta}), 7.49 (7H, m, PPh^{para} with obscured H^5), 7.63 (12H, m, PPh^{ortho}), 7.69 (1H, d, ^3J = 6.4 Hz, H^6). ^{13}C {^1H} NMR (CD_2Cl_2, 20°C): δ = 45.4 (s, NMe), 128.9 (m, PPh^{meta}), 129.3 (m, PPh^{ipso}), 131.5 (s, PPh^{para}), 134.6 (t, $^3J_{CP}$ = 3.7 Hz, C^5), 134.8 (m, PPh^{ortho}), 136.7 (t, $^3J_{CP}$ = 3.7 Hz, C^3), 139.2 (s, C^2), 140.0 (s, C^6), 202.3 (t, $^2J_{CP}$ = 6.1 Hz, C^4), CF_3 not observed. ^{31}P

{^{1}H} NMR (CD_2Cl_2, 20°C): δ = 23.6 (s, PPh_3). MS (FAB): *m/z* (%) = 794.0 (41) [M-CF_3SO_3]$^+$, (^{35}Cl, ^{106}Pd); 758.6 (4) [M-Cl-CF_3SO_3]$^+$; 531.9 (46) [M-PPh_3-CF_3SO_3]$^+$; 496.2 (8) [M-Cl-PPh_3-CF_3SO_3]$^+$. Anal. Calc. for $C_{43}H_{36}NO_3P_2SCl_2F_3Pd$ (943.09 g·mol^{-1}): C 54.76; H 3.85; N 1.49. Found: C 54.57; H 3.78; N 1.55.

***trans*-Chloro(2-chloro-1,4-dihydro-4-pyridylidene)-bis(triphenylphosphine)-palladium(II) triflate.**

According to procedure C: No pure material could be obtained. NMR signals of the main product are overlapping with signals from impurities, thus shifts were unequivocally assigned by gHSQC and gHMQC measurements.

^{1}H NMR (CD_2Cl_2, 20°C): δ = 7.15 (s, H^3), 7.18 (H^6), 7.37 (H^5), 7. 41 (m, PPh^{meta}), 7. 50 (m, PPh^{para}), 7. 63 (m, PPh^{ortho}), NH not observed. ^{13}C {^{1}H} NMR (CD_2Cl_2, 20°C): δ = 128.9 (m, PPh^{meta}), 129.2 (m, PPh^{ipso}), 131.7 (s, PPh^{para}), 133.2 (t, $^3J_{CP}$ = 3.6 Hz, C^5), 134.6 (s, C^6), 134.7 (m, PPh^{ortho}), 135.3 (t, $^3J_{CP}$ = 4.3 Hz, C^3), 137.4 (s, C^2), 204.6 (t, $^2J_{CP}$ = 6.1 Hz, C^4), CF_3 not observed. ^{31}P {^{1}H} NMR (CD_2Cl_2, 20°C): δ = 24.0 (s, PPh_3). MS (FAB): *m/z* (%) = 780.3 (6) [M-CF_3SO_3]$^+$, (^{35}Cl, ^{106}Pd); 744.5 (3) [M-Cl-CF_3SO_3]$^+$; 482.2 (15) [M-Cl-PPh_3-CF_3SO_3]$^+$; 446.2 (3) [M-2Cl-PPh_3-CF_3SO_3]$^+$.

***trans*-Chloro(2-chloro-4-hydro-1-methyl-4-pyridylidene)-bis(triphenylphosphine)nickel(II) triflate, 7.**

According to procedure D: 62.4 % yield of yellow crystals; m.p.(dec.): 160 °C. ^{1}H NMR (CD_2Cl_2, 20°C): δ = 3.71 (3H, s, NMe), 7.16 (1H, bs, H^3), 7.41 (12H, m, PPh^{meta}), 7.48 (7H, m, PPh^{para} with obscured H^6), 7.69 (12H, m, PPh^{ortho}), 7.76 (1H, d, ^{3}J = 6.4 Hz, H^5). ^{13}C {^{1}H} NMR (CD_2Cl_2, 20°C): δ = 45.0 (s, NMe), 128.9 (m, PPh^{meta}), 129.4 (m, PPh^{ipso}), 131.5 (s, PPh^{para}), 133.8 (s, C^5), 134.7 (m, PPh^{ortho}), 136.6 (s, C^3), 136.8 (s, C^6), 136.9 (s, C^2), 210.8 (s, C^4), CF_3 not observed. ^{31}P {^{1}H} NMR (CD_2Cl_2, 20°C): δ = 22.5 (s, PPh_3). MS (FAB): *m/z* (%) = 746.3 (40) [M-CF_3SO_3]$^+$, (^{35}Cl, ^{58}Ni); 710.8 (9) [M-Cl-CF_3SO_3]$^+$; 484.0 (12) [M-PPh_3-CF_3SO_3]$^+$. Anal. Calc. for $C_{43}H_{36}NO_3P_2SCl_2F_3Ni$ (895.36 g·mol^{-1}): C 57.68; H 4.05; N 1.56. Found: C 57.45; H 4.20; N 1.49.

4,7-dichloro-1-methylquinolinium triflate, 8a.

According to procedure A: 99.0 % yield of colourless micro-crystalline material; m.p.: 108 – 111 °C. ^{1}H NMR (CD_2Cl_2, 20°C): δ = 4.65 (3H, s, NMe), 8.03 (1H, dd, $^3J = 9.0$ Hz, $^4J = 1.8$ Hz, H^6), 8.12 (1H, d, $^3J = 6.5$ Hz, H^3), 8.36 (1H, d, $^4J = 1.8$ Hz, H^8), 8.56 (1H, d, $^3J = 9.0$ Hz, H^5), 9.44 (1H, d, $^3J = 6.5$ Hz, H^2). ^{13}C {^{1}H} NMR (CD_2Cl_2, 20°C): δ = 46.4 (s, NMe), 119.1 (s, C^8), 123.2 (s, C^3), 126.8 (s, C^{10}), 128.7 (s, C^5), 132.7 (s, C^6), 139.9 (s, C^9), 144.4 (s, C^7), 151.2 (s, C^2), 154.6 (s, C^4), CF_3 not observed. MS (FAB): *m/z* (%) = 214.0 (69) $[M\text{-}CF_3SO_3]^+$, (^{37}Cl); 212.0 (100) $[M\text{-}CF_3SO_3]^+$, (^{35}Cl). Anal. Calc. for $C_{11}H_8NO_3SCl_2F_3$ (362.15 g·mol^{-1}): C 36.48, H 2.23, N 3.87. Found: C 36.26, H 2.29, N 3.78.

4,7-dichloro-1-hydroquinolinium triflate, 8b.

According to procedure B: 98.0 % yield of colourless micro-crystalline material; m.p.: 146.4 – 147.2 °C. ^{1}H NMR (CD_2Cl_2, 20°C): δ = 8.00 (1H, dd, $^3J = 9.0$ Hz, $^4J = 2.0$ Hz, H^6), 8.08 (1H, d, $^3J = 6.0$ Hz, H^3), 8.47 (2H, m, H^5 and H^8), 9.10 (1H, d, $^3J = 6.0$ Hz, H^2), not observed NH.^{13}C {^{1}H} NMR (CD_2Cl_2, 20°C): δ = 121.3 (s, C^8), 122.8 (s, C^3), 126.4 (s, C^{10}), 127.3 (s, C^5), 133.2 (s, C^6), 139.1 (s, C^9), 143.9 (s, C^7), 155.1 (s, C^2), 145.1 (s, C^4), CF_3 not observed. MS (FAB): *m/z* (%) = 198.0 (100) $[M\text{-}H\text{-}CF_3SO_3]^+$, (^{35}Cl). Anal. Calc. for $C_{10}H_6NO_3SCl_2F_3$ (348.13 g·mol^{-1}): C 34.50, H 1.74, N 4.02. Found: C 34.28, H 1.81, N 4.12.

***trans*-Chloro(7-chloro-4-hydro-1-methyl-4-quinolylidene)-bis(triphenylphosphine)palladium(II) triflate, 9a.**

According to procedure C: 62.9 % yield of colourless crystals; m.p.(dec.): 204 °C. ^{1}H NMR (CD_2Cl_2, 20°C): δ = 4.03 (3H, s, NMe), 7.28 (12H, m, PPh^{meta}), 7.40 (6H, m, PPh^{para}), 7.54 (14H, m, PPh^{ortho} with obscured H^6 and H^8), 7.64 (1H, d, $^3J = 6.4$ Hz, H^3), 7.95 (1H, d, $^3J = 6.4$ Hz, H^5), 8.74 (1H, d, $^3J = 8.8$ Hz, H^2). ^{13}C {^{1}H} NMR (CD_2Cl_2, 20°C): δ = 43.5 (s, NMe), 117.2 (s, C^8), 128.7 (m, PPh^{meta}), 129.3 (m, PPh^{ipso} with C^6), 130.6 (t, $^3J_{CP} = 3.6$ Hz, C^3), 131.4 (s, PPh^{para}), 134.5 (bs, C^{10}), 134.6 (m, PPh^{ortho}), 135.1 (s, C^9), 137.0 (s, C^5), 141.2 (s, C^7), 141.8 (s, C^2), 206.6 (t, $^2J_{CP} = 5.5$ Hz, C^4), CF_3 not observed. ^{31}P {^{1}H} NMR (CD_2Cl_2, 20°C): δ = 23.2 (s, PPh_3). MS (FAB): *m/z* (%) = 844.0

(74) [M-CF_3SO_3]$^+$, (^{35}Cl, ^{106}Pd); 581.9 (100) [M- PPh_3-CF_3SO_3]$^+$; 546.0 (13) [M-Cl-PPh_3-CF_3SO_3]$^+$; 404.1 (54) [M-L-PPh_3-CF_3SO_3]$^+$. Anal. Calc. for $C_{47}H_{38}NO_3P_2SCl_2F_3Pd$ (993.14 g·mol^{-1}): C 56.84; H 3.86; N 1.41. Found: C 56.66; H 3.99; N 1.32.

***trans*-Chloro(7-chloro-1,4-dihydro-4-quinolylidene)-bis(triphenylphosphine)-palladium(II) triflate, 9b.**

According to procedure C: 85.3 % yield of colourless micro-crystalline material; m.p.(dec.): 207 °C. ^{1}H NMR (CD_2Cl_2, 20°C): δ = 7.27 (12H, m, PPh), 7.41 (6H, m, PPh), 7.43 (1H, dd, ^3J = 8.8 Hz, ^4J = 2.0 Hz, H^6), 7.49 (1H, d, ^3J = 5.8 Hz, H^2), 7.52, (13H, m, PPh with obscured H^3), 7.69 (1H, d, ^4J = 2.0 Hz, H^8), 8.55 (1H, d, ^3J = 8.8 Hz, H^5), not observed NH. ^{13}C {^{1}H} NMR (CD_2Cl_2, 20°C): δ = 120.2 (s, C^8), 128.7 (m, PPh^{meta}), 129.2 (m, PPh^{ipso}), 129.3 (s, C^6), 129.4 (s, C^9), 129.6 (t, $^3J_{CP}$ = 4.3 Hz, C^3), 131.5 (s, PPh^{para}), 133.8 (t, $^3J_{CP}$ = 2.5 Hz, C^{10}), 134.5 (m, PPh^{ortho}), 135.2 (s, C^5), 135.6 (s, C^2), 140.2 (s, C^7), 207.2 (t, $^2J_{CP}$ = 5.5 Hz, C^4), CF_3 not observed. ^{31}P {^{1}H} NMR (CD_2Cl_2, 20°C): δ = 23.8 (s, PPh_3). MS (FAB): *m/z* (%) = 830.4 (5) [M-CF_3SO_3]$^+$, (^{35}Cl, ^{106}Pd); 794.5 (1) [M-Cl-CF_3SO_3]$^+$; 568.3 (5) [M-PPh_3-CF_3SO_3]$^+$; 532.3 (1) [M-Cl-PPh_3-CF_3SO_3]$^+$. Anal. Calc. for $C_{46}H_{36}NO_3P_2SCl_2F_3Pd$ (979.12 g·mol^{-1}): C 56.43, H 3.71, N 1.43. Found: C 56.22, H 3.87, N 1.46.

***trans*-Chloro(7-chloro-4-hydro-1-methyl-4-quinolylidene)-bis(triphenylphosphine)nickel(II) triflate, 10a.**

According to procedure D: 80.4 % yield of yellow crystals; m.p.(dec.): 176 °C. ^{1}H NMR (CD_2Cl_2, 20°C): δ = 3.90 (3H, s, NMe), 7.29 (12H, m, PPh^{meta}), 7.42 (7H, m, PPh^{para} with obscured H^8), 7.59 (13H, m, PPh^{ortho} with obscured H^6), 7.66 (1H, d, ^3J = 6.3 Hz, H^3), 7.89 (1H, d, ^3J = 6.3 Hz, H^5), 9.44 (1H, d, ^3J = 8.8 Hz, H^2). ^{13}C {^{1}H} NMR (CD_2Cl_2, 20°C): δ = 43.0 (s, NMe), 117.2 (s, C^8), 128.6 (m, PPh^{meta}), 128.8 (s, C^6), 129.3 (m, PPh^{ipso}), 130.6 (bs, C^3), 131.2 (s, PPh^{para}), 133.3 (s, C^9), 134.6 (m, PPh^{ortho}), 135.3 (s, C^{10}), 136.6 (s, C^5), 137.9 (s, C^2), 140.9 (s, C^7), 216.7 (t, $^2J_{CP}$ = 30.5 Hz, C^4), CF_3 not observed. ^{31}P {^{1}H} NMR (CD_2Cl_2, 20°C): δ = 21.9 (s, PPh_3). MS (FAB): *m/z* (%) = 796.2 (19) [M-CF_3SO_3]$^+$, (^{35}Cl, ^{58}Ni); 533.9 (68) [M-PPh_3-CF_3SO_3]$^+$. Anal. Calc. for

$C_{47}H_{38}NO_3P_2SCl_2F_3Ni$ (945.42 g·mol^{-1}): C 59.71; H 4.05; N 1.48. Found: C 60.07; H 4.26; N 1.39.

***trans*-Chloro(7-chloro-1,4-dihydro-4-quinolylidene)bis(triphenylphosphine)nickel(II) triflate, 10b.**

According to procedure D: 68.1 % yield of yellow crystals; m.p.(dec.): 197 °C. ^{1}H NMR (CD^2Cl^2, 20°C): δ = 7.28 (13H, m, PPh with obscured H^3), 7.40 (6H, m, PPh), 7.48 (1H, dd, ^3J = 8.8 Hz, ^4J = 1.9 Hz, H^6), 7.55 (13H, m, PPh with obscured H^8), 7.77 (1H, d, ^3J = 5.8 Hz, H^2), 9.19 (1H, d, ^3J = 8.8 Hz, H^5), not observed NH. ^{13}C {^{1}H} NMR (CD_2Cl_2, 20°C): δ = 120.3 (s, C^8), 128.6 (m, PPh^{meta}), 128.7 (s, C^6), 129.3 (m, PPh^{ipso}), 129.6 (t, $^3J_{CP}$ = 3.7 Hz, C^3), 131.3 (s, PPh^{para}), 132.0 (s, C^2), 132.0 (s, C^9), 134.4 (m, PPh^{ortho}), 134.7 (bs, C^{10}), 134.9 (s, C^5), 140.0 (s, C^7), 216.6 (t, $^2J_{CP}$ = 30.0 Hz, C^4), CF_3 not observed. ^{31}P {^{1}H} NMR (CD_2Cl_2, 20°C): δ = 22.6 (s, PPh_3). MS (FAB): *m/z* (%) = 782.1 (3) $[M-CF_3SO_3]^+$, (^{35}Cl, ^{58}Ni); 746.9 (1) $[M-Cl-CF_3SO_3]^+$; 520.0 (10) $[M-Cl-PPh_3-CF_3SO_3]^+$. Anal. Calc. for $C_{46}H_{36}NO_3P_2SCl_2F_3Ni$ (931.39 g·mol^{-1}): C 59.32, H 3.90, N 1.50. Found: C 59.11, H 4.02, N 1.63.

Typical Procedure for the Suzuki-Miyaura coupling

The reactions were performed under inert conditions using dry and degassed reagents. Phenylboronic acid (3 mmol, 0.3658 g), bromo acetophenone (2 mmol, 0.3981 g), potassium carbonate/cesium carbonate (4 mmol, 0.5528/1.303 g), diethyleneglycol-di-n-butylether (2 mmol, 0.4367 g, 0.5 ml) and dimethylacetamide (5 ml) were placed in a 25 ml three-neck round bottom flask. The flask was connected to N_2, equipped with a reflux condenser and a septum. The catalyst solution was added after heating to 130°C. Aliquots (0.2 ml) were taken at regular intervals from the reaction mixture and added to 5ml of CH_2Cl_2. The organic layer was washed with 3 x 5 ml of water, dried over MgSO4 and filtered. The solvent was removed *in vacuo* and the residue was analysed by ^{1}H NMR spectroscopy.

Crystal Structure Determinations

Data associated with the crystal structures are summarized in Tables 4 and 1S(upporting Informations). Intensity data were collected at T = 100 K with a Bruker SMART Apex diffractometer with graphite-monochromated Mo-K_α radiation (λ = 0.71073 Å). Intensities were measured using the ω-scan mode and were corrected for Lorentz and polarization effects.[76-79] The structures were solved by direct methods (SHELXS-97) and refined by full-matrix least-squares on F^2 (SHELXL-97).[80] Non-hydrogen atoms were refined with anisotropic displacement parameters. Hydrogen atoms were placed in idealized positions and refined using a riding model with fixed isotropic contributions if possible. Reinvestigation of the crystal data of **3b** (in the BF_4 salt - previously published)[20] yielded a so far unnoticed disorder (s.o.f.: 0.2) of the carbene ligand. Refinement of the less occupied site was supported by restraining its geometry to fit the major ligand site using SAME. All crystals were found to contain solvent. In **3b**, **4b** and **9a** the dicholormethane molecules could not be resolved due to disorder and were thus removed by the SQUEEZE routine in PLATON.[81] Detailed information about the solvent accessible void and removed electrons can be found in the CIF along with a complete lists of displacement parameters and tables of interatomic distances and angles. These have been deposited with the Cambridge Crystallographic Data Centre and can be obtained free of charge via www.ccdc.cam.ac.uk/data_request/cif on quoting CCDS-XXXXX.

Table 4. Crystal Data, Data Collection and Structure Refinement Details

	3b	**4b**
Empirical formula	$C_{42}H_{37}ClNP_2Pd \cdot CF_3O_3S$	$C_{42}H_{37}ClNNiP_2 \cdot CF_3O_3S$
M_r	908.59	860.90
Crystal system	Monoclinic	Monoclinic
Space group	$P2(1)/n$	$P2(1)/n$
a/Å	14.672 (5)	14.6778 (18)
b/Å	18.609 (6)	18.491 (2)
c/Å	18.404 (6)	18.317 (2)
α/°	90	90
β/°	107.724 (5)	109.068 (2)
γ/°	90	90
V/Å^3	4786 (3)	4698.6 (10)
ρ_{calc}/g cm^{-3}	1.261	1.217
Z	4	4
$F(000)$	1848	1776
μ (Mo-K$_\alpha$) (mm^{-1})	0.60	0.63
T/K	100	100
Refls. measured	24537	23577
Refls. unique	8709 [R_{int} = 0.117]	8384 [R_{int} = 0.031]
Refined param. /restraints	497 / 1	497 / 0
$R1$ [$I \geq 2\sigma(I)$]	0.068	0.042
$wR2$[a]	0.181	0.113
Weighting scheme[a]	a = 0.0896 b = 0.000	a = 0.0617 b = 0.1765
σ_{fin}(max/min)/eÅ^{-3}	1.34 / −1.50	0.66 / −0.33

[a] $wR2 = \{\Sigma[w(F_o^2 - F_c^2)^2]/\Sigma[w(F_o^2)^2]\}^{1/2}$; $w = 1/[\sigma^2(F_o^2)+(ap)^2+bp]$; $p = (F_o^2 + 2F_c^2)/3$

Table 4. (continued)

	6·2CH$_2$Cl$_2$	**7**·CH$_2$Cl$_2$	**9a**
Empirical formula	$C_{42}H_{36}Cl_2NP_2Pd$ $\cdot CF_3O_3S\cdot 2(CH_2Cl_2)$	$C_{42}H_{36}Cl_2NNiP_2$ $\cdot CF_3O_3S\cdot CH_2Cl_2$	$C_{46}H_{38}Cl_2NP_2Pd\cdot CF_3O_3S$
M_r	1112.88	980.26	993.08
Crystal system	Monoclinic	Monoclinic	Monoclinic
Space group	*P*2(1)/*c*	*P*2(1)/*n*	C2/c
a/Å	17.6792 (17)	10.5898 (7)	25.183 (6)
b/Å	16.9370 (17)	21.8258 (14)	11.472 (2)
c/Å	16.3414 (16)	19.7422 (13)	34.952 (7)
α/°	90	90	90
β/°	106.954 (2)	104.7130 (10)	99.278 (4)
γ/°	90	90	90
V/Å^3	4680.5 (8)	4413.4 (5)	9966 (4)
ρ_{calc}/g cm^{-3}	1.579	1.475	1.324
Z	4	4	8
F(000)	2248	2008	4032
μ (Mo-K$_\alpha$) (mm^{-1})	0.91	0.86	0.63
T/K	100	100	100
Refls. measured	24156	23126	26296
Refls. unique	731 [R_{int} = 0.034]	8048 [R_{int} = 0.028]	9103 [R_{int} = 0.047]
Refined param. /restraints	560 / 0	533/ 0	542 / 2
*R*1 [I≥2σ(I)]	0.053	0.038	0.042
*wR*2^a	0.120	0.095	0.097
Weighting scheme^a	a = 0.0457 b = 17.9112	a = 0.048 b = 3.1369	a = 0.0534 b = 0.000
σ_{fin}(max/min)/eÅ^{-3}	1.67 / −1.56	0.72 / −0.59	0.91/ −0.54

^{a} $wR2 = \{\Sigma[w(F_o^2-F_c^2)^2]/\Sigma[w(F_o^2)^2]\}^{1/2}$; $w = 1/[\sigma^2(F_o^2)+(ap)^2+bp]$; $p = (F_o^2+2F_c^2)/3$

Computational Section

All geometries were optimized under C_s-symmetry constraint using density functional theory at the BP86 level of theory[82,83] using uncontracted Slater-type orbitals (STOs) with TZ2P quality as basis functions for the SCF calculations.[84] An auxiliary set of s, p, d, f, and g STOs was used to fit the molecular densities and to represent the Coulomb and exchange potentials accurately in each SCF cycle.[85] Scalar relativistic effects have been incorporated by applying the zeroth-order regular approximation (ZORA).[86] The nature of the stationary points on the potential energy surface was determined by calculating the vibrational frequencies. All structures are minima on the potential energy surface (PES).

The bonding situation of the metal-carbene bonds was investigated by an energy decomposition analysis (EDA) which was developed by Morokuma[87] and by Ziegler and Rauk.[88,89] The bonding analysis focuses on the instantaneous interaction energy ΔE_{int} of a bond A-B between two fragments A and B in the particular electronic reference state and in the frozen geometry of AB. This interaction energy is divided into three main components [Eq. (1)].

$$\Delta E_{int} = \Delta E_{elstat} + \Delta E_{Pauli} + \Delta E_{orb} \qquad (1)$$

The term ΔE_{elstat} corresponds to the classical electrostatic interaction between the unperturbed charge distributions of the prepared atoms and is usually attractive. The Pauli repulsion ΔE_{Pauli} is the energy change associated with the transformation from the superposition of the unperturbed electron densities $\rho_A + \rho_B$ of the isolated fragments to the wavefunction $\Psi^0 = N\hat{A}[\Psi_A \Psi_B]$, which properly obeys the Pauli principle through explicit antisymmetrization ($\hat{A}$ operator) and renormalization of the product wavefunction.[90] It comprises the destabilizing interactions between electrons of the same spin on either fragment. The orbital interaction ΔE_{orb} accounts for charge transfer and polarization effects.[91] The ΔE_{orb} term can be decomposed into contributions from each irreducible representation of the point group of the interacting system. This makes it possible to estimate the intrinsic strength of orbital interactions from orbitals having a’ (σ) and a'' (π) symmetry quantitatively. To obtain the bond dissociation energy (BDE) D_e the preparation energy ΔE_{prep} which gives the relaxation of the fragments into their electronic and geometrical ground states must be added to ΔE_{int} [Eq. (2)].

$$\Delta E(= -D_e) = \Delta E_{int} + \Delta E_{prep} \qquad (2)$$

To calculate the dissociation energies, we calculated each fragment in its optimized geometry and derived ΔE by equation (2). Further details on the EDA can be found in the literature.[90,92] The EDA has been used by us for a comprehensive study of metal-ligand interactions in transition metal complexes.[93,94]

Supporting Information Available:

Crystallographic details as CIF; ORTEP figure of **3a** (in the BF_4 salt) with resolved disorder; correlation of calculated charges and ^{13}C NMR data in chloropyridines; average geometries of chloropyridinium salts; cartesian coordinates for all calculated structures. This material is available free of charge via the Internet at http://pubs.acs.org.

Acknowledgements

We are very grateful to Dr. Ralf Tonner whose additional calculations helped to settle questions that arose during the peer-review process. We also thank the South African National Research Foundation for financial support. ES thanks SASOL for a PhD scholarship, OS, SC and HGR appreciate support from the Alexander von Humboldt Foundation and OS from the German Academy of Sciences Leopoldina (BMBF LPD 9901/8-179). GH further thanks the DAAD (Grant number A/05/52686) for post-doctoral funding. MA is very grateful for an Alfred Werner Assistant Professorship.

References

(1) Bertrand (ed.), G. *J. Organomet. Chem.* **2005**, *690(24-25)*.

(2) Crabtree (ed.), R. H. *Coord. Chem. Rev.* **2007**, *251(5-6)*.

(3) Glorius (ed.), F. *Top. Organomet. Chem.* **2007**, *21*.

(4) Nolan, S. P. *N-Heterocyclic Carbenes in Synthesis*; Wiley-VCH: Weinheim, 2006.

(5) Hahn, F. E.; Jahnke, M. C. *Angew. Chem., Int. Ed.* **2008**, *47*, 3122.

(6) Gruendemann, S.; Kovacevic, A.; Albrecht, M.; Faller, J. W.; Crabtree, R. H. *Chem. Commun.* **2001**, 2274.

(7) Gruendemann, S.; Kovacevic, A.; Albrecht, M.; Faller, J. W.; Crabtree, R. H. *J. Am. Chem. Soc.* **2002**, *124*, 10473.

(8) Kluser, E.; Neels, A.; Albrecht, M. *Chem. Commun.* **2006**, 4495.

(9) Heckenroth, M.; Kluser, E.; Neels, A.; Albrecht, M. *Angew. Chem., Int. Ed.* **2007**, *46*, 6293.

(10) Tonner, R.; Heydenrych, G.; Frenking, G. *Chem-Asian J* **2007**, *2*, 1555.

(11) Tonner, R.; Heydenrych, G.; Frenking, G. *ChemPhysChem* **2008**, *9*, 1474.

(12) Yang, L.; Kruger, A.; Neels, A.; Albrecht, M. *Organometallics* **2008**, *27*, 3161.

(13) Albrecht, M. *Chem. Commun.* **2008**, 3601.

(14) Heckenroth, M.; Albrecht, M. *Chimia* **2008**, *62*, 253.

(15) Heckenroth, M.; Kluser, E.; Neels, A.; Albrecht, M. *Dalton Trans.* **2008**, 6242.

(16) Heckenroth, M.; Neels, A.; Garnier, M. G.; Aebi, P.; Ehlers, A. W.; Albrecht, M. *Chem-Eur J* **2009**, *15*, 9375.

(17) Aldeco-Perez, E.; Rosenthal, A. J.; Donnadieu, B.; Parameswaran, P.; Frenking, G.; Bertrand, G. *Science* **2009**, *326*, 556.

(18) Schuster, O.; Yang, L.; Raubenheimer, H. G.; Albrecht, M. *Chem. Rev.* **2009**, *109*, 3445.

(19) Raubenheimer, H. G.; Toerien, J. G.; Kruger, G. J.; Otte, R.; van Zyl, W.; Olivier, P. *J. Organomet. Chem.* **1994**, *466*, 291.

(20) Schneider, S. K.; Roembke, P.; Julius, G. R.; Raubenheimer, H. G.; Herrmann, W. A. *Adv. Synth. Catal.* **2006**, *348*, 1862.

(21) Schneider, S. K.; Julius, G. R.; Loschen, C.; Raubenheimer, H. G.; Frenking, G.; Herrmann, W. A. *Dalton Trans.* **2006**, 1226.

(22) Schneider, S. K.; Rentzsch, C. F.; Krueger, A.; Raubenheimer, H. G.; Herrmann, W. A. *J Mol Catal A-Chem* **2007**, *265*, 50.

(23) Raubenheimer, H. G.; Cronje, S. *Dalton Trans.* **2008**, 1265.

(24) Heydenrych, G.; von Hopffgarten, M.; Stander, E.; Schuster, O.; Raubenheimer, H. G.; Frenking, G. *Eur. J. Inorg. Chem.* **2009**, 1892.

(25) Strasser, C. E.; Stander-Grobler, E.; Schuster, O.; Cronje, S.; Raubenheimer, H. G. *Eur. J. Inorg. Chem.* **2009**, 1905.

(26) Lavorato, D. J.; Terlouw, J. K.; Dargel, T. K.; Koch, W.; McGibbon, G. A.; Schwarz, H. *J. Am. Chem. Soc.* **1996**, *118*, 11898.

(27) Lavorato, D. J.; Terlouw, J. K.; McGibbon, G. A.; Dargel, T. K.; Koch, W.; Schwarz, H. *Int. J. Mass Spectrom.* **1998**, *180*, 7.

(28) Kassaee, M. Z.; Shakib, F. A.; Momeni, M. R.; Ghambarian, M.; Musavi, S. M. *Tetrahedron* **2009**, *65*, 10093.

(29) Holloczki, O.; Nyulaszi, L. *J. Org. Chem.* **2008**, *73*, 4794.

(30) Weisman, A.; Gozin, M.; Kraatz, H. B.; Milstein, D. *Inorg. Chem.* **1996**, *35*, 1792.

(31) Cave, G. W. V.; Hallett, A. J.; Errington, W.; Rourke, J. P. *Angew. Chem., Int. Ed.* **1998**, *37*, 3270.

(32) Newman, C. P.; Clarkson, G. J.; Alcock, N. W.; Rourke, J. P. *Dalton Trans.* **2006**, 3321.

(33) Alvarez, E.; Conejero, S.; Paneque, M.; Petronilho, A.; Poveda, M. L.; Serrano, O.; Carmona, E. *J. Am. Chem. Soc.* **2006**, *128*, 13060.

(34) Alvarez, E.; Conejero, S.; Lara, P.; Lopez, J. A.; Paneque, M.; Petronilho, A.; Poveda, M. L.; del Rio, D.; Serrano, O.; Carmona, E. *J. Am. Chem. Soc.* **2007**, *129*, 14130.

(35) Cordone, R.; Harman, W. D.; Taube, H. *J. Am. Chem. Soc.* **1989**, *111*, 2896.

(36) Koizumi, T.; Tomon, T.; Tanaka, K. *Organometallics* **2003**, *22*, 970.

(37) Koizumi, T.; Tomon, T.; Tanaka, K. *J. Organomet. Chem.* **2005**, *690*, 1258.

(38) Albrecht, M.; Stoeckli-Evans, H. *Chem. Commun.* **2005**, 4705.

(39) Koizumi, T.; Tomon, T.; Tanaka, K. *J. Organomet. Chem.* **2005**, *690*, 4272.

(40) Meyer, W. H.; Deetlefs, M.; Pohlmann, M.; Scholz, R.; Esterhuysen, M. W.; Julius, G. R.; Raubenheimer, H. G. *Dalton Trans.* **2004**, 413.

(41) Schneider, S. K.; Roembke, P.; Julius, G. R.; Loschen, C.; Raubenheimer, H. G.; Frenking, G.; Herrmann, W. A. *Eur. J. Inorg. Chem.* **2005**, 2973.

(42) Schuster, O.; Raubenheimer, H. G. *Inorg. Chem.* **2006**, 7997.

(43) As a possible indicator for a hindered rotation around the metal carbon bond and hence an increased metal-carbon bond order, we investigated the angles between the mean square planes of the pyridylidene ring and the coordination spheres. Given the fact that an in-plane arrangement is prevented by the bulky phosphine ligands, efficient π backbonding should result in an orthogonal alignment. Notably, both 4-pyridylidene ligands in the two complexes **3c** and **4c** deviate considerably from this ideal geometry. We are however hesitant to ascribe this

observation to an electronic effect because steric considerations seem to prevail (*cf.* supporting information).

(44) Jonas, V.; Frenking, G.; Reetz, M. T. *J. Am. Chem. Soc* **1994**, *116*, 8741.

(45) Owen, J. S.; Labinger, J. A.; Bercaw, J. E. *J. Am. Chem. Soc.* **2004**, *126*, 8247.

(46) We mention that reinvestigation of the crystal structure of **3a (**in the tetrafluoroborate salt) revealed disorder of the pyridylidene ligand (s.o.f. 20) which was not found when the result was published initially.{Schneider et al., 2006, #246} The updated structure and selected data can be found in the supporting information. However, the disorder compromises a closer examination of the bond distances and angles in the carbene ligand and we shall therefore concentrate on the nickel complexes which also, in general, offered better data.

(47) Conejero, S.; Lara, P.; Paneque, M.; Petronilho, A.; Poveda, M. L.; Serrano, O.; Vattier, F.; Alvarez, E.; Maya, C.; Salazar, V.; Carmona, E. *Angew. Chem., Int. Ed.* **2008**, *47*, 4380.

(48) Bruno, I. J.; Cole, J. C.; Edgington, P. R.; Kessler, M.; Macrae, C. F.; McCabe, P.; Pearson, J.; Taylor, R. *Acta Crystallogr., Sect. B: Struct. Sci.* **2002**, *58*, 389.

(49) Meguro, H.; Koizumi, T.; Yamamoto, T.; Kanbara, T. *J. Organomet. Chem.* **2008**, *693*, 1109.

(50) Isobe, K.; Nakamura, Y.; Miwa, T.; Kawaguchi, S. *Bull. Chem. Soc. Jpn.* **1987**, *60*, 149.

(51) Crociani, B.; Di Bianca, F.; Giovenco, A.; Berton, A.; Bertani, R. *J. Organomet. Chem.* **1989**, *361*, 255.

(52) Crociani, B.; Di Bianca, F.; Fontana, A.; Bertani, R. *J. Organomet. Chem.* **1992**, *425*, 155.

(53) Canovese, L.; Uguagliati, P.; Bianca, F. D.; Crociani, B. *J. Organomet. Chem.* **1992**, *438*, 253.

(54) Crociani, B.; Di Bianca, F.; Fontana, A.; Forsellini, E.; Bombieri, G. *J. Chem. Soc., Dalton Trans.* **1994**, 407.

(55) Canovese, L.; Visentin, F.; Uguagliati, P.; Di Bianca, F.; Fontana, A.; Crociani, B. *J. Organomet. Chem.* **1996**, *525*, 43.

(56) Lauterbur, P. C. *Tetrahedron Lett.* **1961**, *2*, 274.

(57) Retcofsky, H. L.; McDonald, F. R. *Tetrahedror. Letters* **1968**, 2575.

(58) Hesse, M.; Meier, H.; Zeeh, B. *Spectroscopic Methods in Organic Chemistry*; Thieme, 2008.

(59) Lauterbur, P. C. *J. Chem. Phys.* **1965**, *43*, 360.

(60) Isobe, K.; Kai, E.; Nakamura, Y.; Nishimoto, K.; Miwa, T.; Kawaguchi, S.; Kinoshita, K.; Nakatsu, K. *J. Am. Chem. Soc.* **1980**, *102*, 2475.

(61) Spiesecke, H.; Schneider, W. G. *J. Chem. Phys.* **1961**, *35*, 722.

(62) Kutzelnigg, W. *Isr. J. Chem.* **1980**, *19*, 193.

(63) Kutzelnigg, W.; Fleischer, U.; Schindler, M. *Basic Princ. Prog.* **1990**, *23*, 165.

(64) Feshin, V. P.; Feshina, E. V.; Zhizhina, L. I. *J. Het. Chem.* **2006**, *42*, 1435.

(65) Wehrli, F. W.; Giger, W.; Simon, W. *Helv. Chim. Acta* **1971**, *54*, 229.

(66) Pugmire, R. J.; Grant, D. M. *J. Am. Chem. Soc.* **1968**, *90*, 697.

(67) Tukov, A. A.; Normand, A. T.; Nechaev, M. S. *Dalton Trans.* **2009**, 7015.

(68) Iglesias, M.; Albrecht, M. **2010**, *39*, in press (DOI: 10.1039/c0dt00027b).

(69) Test reactions under Buchwald-Hartwig conditions yielded palladium black even at very low temperatures and no discrimination between the precatalysts **3** with Pd(OAc)2 or PdCl2 was possible - probably due to a predominantly heterogeneous mode of action.

(70) Schroter, S.; Stock, C.; Bach, T. *Tetrahedron* **2005**, *61*, 2245.

(71) Fitton, P.; Rick, E. A. *J. Organomet. Chem.* **1971**, *28*, 287.

(72) Portnoy, M.; Milstein, D. *Organometallics* **1993**, *12*, 1665.

(73) Senn, H. M.; Ziegler, T. *Organometallics* **2004**, *23*, 2980.

(74) Sicre, C.; Alonso-Gomez, J.; Cid, M. M. *Tetrahedron* **2006**, *62*, 11063.

(75) Ozawa, F. In *Synthesis of Organometallic Compounds*; Komiya, S., Ed.; John Wiley & Sons: Chichester, 1997.

(76) SADABS (version 2.05), Bruker AXS Inc., Madison, WI, **2002**.

(77) SAINT: Data reduction software (version 6.45), Bruker AXS Inc., Madison, WI, **2003**.

(78) SMART: Data collection software (version 5.629), Bruker AXS Inc., Madison, WI, **2003**.

(79) Blessing, R. H. *Acta Crystallogr., Sect. A* **1995**, *51*, 33.

(80) Sheldrick, G. M. *Acta Crystallogr A* **2008**, *64*, 112.

(81) Spek, A. L. *J. Appl. Crystallogr.* **2003**, *36*, 7.

(82) Becke, A. D. *Phys. Rev. A* **1988**, *38*, 3098.

(83) Perdew, J. *Phys. Rev. B: Condens. Matter* **1986**, *34*, 7406.

(84) Snijders, J. G.; Vernooijs, P.; Baerends, E. *At. Data Nucl. Data Tables* **1981**, 483.

(85) Krijn, J.; Baerends, E. J., *Fit Functions in the HFS-Method*, Internal Report (in Dutch), Vrije Universiteit Amsterdam, The Netherlands, **1984**.

(86) vanLenthe, E.; vanLeeuwen, R.; Baerends, E. J.; Snijders, J. G. *Int. J. Quantum Chem.* **1996**, *57*, 281.

(87) Morokuma, K. *J. Chem. Phys.* **1971**, *55*, 1236.

(88) Ziegler, T.; Rauk, A. *Inorg. Chem.* **1979**, *18*, 1755.

(89) Ziegler, T.; Rauk, A. *Inorg. Chem.* **1979**, *18*, 1558.

(90) Bickelhaupt, F. M.; Baerends, E. J. In *Reviews in Computational Chemistry, vol. 15*; Wiley-VCH: New York, 2000.

(91) Bickelhaupt, F. M.; Nibbering, N. M. M.; van Wezenbeek, E. M.; Baerends, E. *J. Phys. Chem.* **1992**, *96*, 4864.

(92) Velde, G. T.; Bickelhaupt, F. M.; Baerends, E.; Guerra, C. F.; Van Gisbergen, S. J. A.; Snijders, J. G.; Ziegler, T. *J. Comput. Chem.* **2001**, *22*, 931.

(93) Frenking, G.; Wichmann, K.; Fröhlich, N.; Loschen, C.; Lein, M.; Frunzke, J.; Rayon, V. M. *Coord. Chem. Rev.* **2003**, *238*, 55.

(94) Lein, M.; Frenking, G. In *Theory and Application of Computational Chemistry: The First Forty Years*; Dykstra, E., Frenking, G., Kim, K. S., Scuseria, G. E., Eds.; Elsevier: Amsterdam, 2005.

TOC - Abstract

On the basis of isomeric complexes with the general formula *trans*-(pyridylidene)M(PPh_3)$_2$Cl (M = Ni, Pd) *normal*, *abnormal* and *remote* bonding of pyridylidenes was systematically investigated.

TOC - Figure